

# ERROR ANALYSIS OF AN ASYMPTOTIC PRESERVING DYNAMICAL LOW-RANK INTEGRATOR FOR THE MULTI-SCALE RADIATIVE TRANSFER EQUATION

ZHIYAN DING, LUKAS EINKEMMER, AND QIN LI

**ABSTRACT.** Dynamical low-rank algorithm are a class of numerical methods that compute low-rank approximations of dynamical systems. This is accomplished by projecting the dynamics onto a low-dimensional manifold and writing the solution directly in terms of the low-rank factors. The approach has been successfully applied to many types of differential equations. Recently, efficient dynamical low-rank algorithms have been applied in [11, 15] to treat kinetic equations, including the Vlasov–Poisson and the Boltzmann equation, where it was demonstrated that the methods are able to capture the low rank structure of the solution and significantly reduce the numerical effort, while often maintaining good accuracy. However, no numerical analysis is currently available.

In this paper, we perform an error analysis for a dynamical low-rank algorithm applied to a classical model in kinetic theory, namely the radiative transfer equation. The model used here includes a small parameter, the Knudsen number. This setting is particularly interesting since the solution is known to be rank one in certain regimes. We will prove that the scheme dynamically and automatically captures the low-rank structure of the solution, and preserves the fluid limit on the numerical level. This work thus serves as the first mathematical error analysis for a dynamical low rank approximation applied to a kinetic problem.

## 1. INTRODUCTION

Kinetic equations are a class of model equations used to describe the statistical behavior of a large number of particles that follow the same physics laws. They have been widely used in many aspects of physics and engineering: the classical Boltzmann equation describes the dynamics of rarefied gases, the radiative transfer equation characterizes the behavior of photons, the neutron transport equation describes the dynamics of neutrons in nuclear reactors, and the Vlasov–Poisson system has been used to describe the motion of plasmas.

These equations, despite there being significant differences for various kinds of particles, share a similar structure. In all situations the dynamics is described in phase space and the solution is thus a distribution function  $u(t, x, v)$  that counts the number of particles at a particular time  $t$ , location  $x$ , and velocity  $v$ . One major reason for kinetic equations being challenging is that they are posed in a higher dimensional space; this is different from most other physical models that describe the corresponding dynamics only on the physical domain, e.g. for a fluid model the solution only depends on  $(t, x)$ .

During the past decade, numerous methods have been proposed to numerically solve kinetic equations and many of them succeed in reducing computational cost without sacrificing accuracy. The main body of work concentrates on developing fast solvers for the collision operators and overcoming the stability requirement via relaxing the time-discretization [24, 22], through either finding fast methods to treat the transport term [17, 44, 5, 12], or implementing the resulting discrete system efficiently [18, 13]. However, reducing the complexity due to the high dimensionality is largely left unaddressed. The difficulty here is rather clear. To numerically

solve kinetic equations, one needs to sample a certain amount of discrete points in each dimension, resulting in a large number of degrees of freedom. The numerical cost, meanwhile, is typically determined mainly by the total number of degrees of freedom.

This viewpoint was challenged in [42] (based on earlier work on very high dimensional systems in quantum mechanics). There the authors abandon the traditional approach. They propose a dynamical low-rank approximation that relies more on the intrinsic dimensionality of the manifold the solution lives on. This method is designed to follow the flow of the dynamics and to identify the important features in the evolution. Since the equation is projected onto a solution manifold of lower dimensionality, only the core information is preserved and some redundant information is thrown away. The numerical cost thus depends mainly on the intrinsic dimensionality of the dynamics, rather than the total number of discrete points. The method was first utilized to deal with coupled ODE systems [36] and it has been demonstrated that, for a range of problems, it can preserve the accuracy of the solution.

The success in dealing with ODE systems inspired the generalization to PDEs. More recently, a class of efficient numerical schemes were proposed for kinetic equations. In the past few years, the method was applied to the Vlasov–Poisson system [28, 15], the Vlasov-Maxwell system [16] and the classical Boltzmann equation [11] in both collisionless and strong-collisional regimes, and it is observed that both the sophisticated Landau damping phenomenon for the VP system [45, 41], and the incompressible Navier-Stokes limit for the Boltzmann equation are captured rather accurately with low cost. Different equations may require slightly modified dynamical low-rank algorithms to suit the specific structures of the equation, but the general approach is quite similar: one looks for the main features in the evolution and follows the flow of the equation projected onto the solution manifold of a certain low rank.

However, despite the strong intuition and the many promising numerical experiments, a mathematical error analysis is largely absent from all of those works (especially in the PDE setting). There are two major difficulties here. First, we often do not have results to show that the true solution is indeed approximately of low-rank. This point is more subtle than one might think. In fact, a Fourier expansion is also a low-rank approximation. But, a Fourier expansion uses a fixed set of basis functions, leading to unnecessary high ranks. In addition, showing low-rank by performing a Fourier decomposition relies on assuming smoothness of the solution, which for kinetic equations is certainly problematic. It should be noted, however, that for elliptic equations some results can be obtained [6].

The second difficulty is that we have to show that the numerical method actually captures the low-rank structure of the solution. For the ODE case an analysis has been performed in [26] and related works, but this analysis only applies to the non-stiff case and is thus not applicable to PDEs. The only mathematical analysis of a dynamical low-rank scheme in the PDE setting we are aware of is found in [43]. This paper considers a special situation where the stiffness originates only from the linear differential operator whose corresponding flow is exactly computable within the low-rank formulation. This separation suggests a splitting procedure that decouples the stiff and non-stiff dynamics, which permits the convergence of the resulting method. This is not the situation for kinetic equations, and thus the analysis does not apply.

The goal of the current paper is therefore to fill this void. In particular, we will consider a multi-scale radiative transfer equation, essentially a linearized Boltzmann equation. For this equation we will propose a dynamical

low-rank algorithm and theoretically justify the validity and efficiency of this method in the strong-collisional regime (small Knudsen number). More specifically, we will show that in the small Knudsen number limit, the method is asymptotic preserving (that is, it correctly approximates the diffusion limit of the radiative transfer equation) and that it automatically captures the corresponding low-rank structure of the solution. It implies that the required degrees of freedom only scale as the number of grid points in physical space, in contrast to the full phase space as is required by other methods. This is, to our knowledge, the first numerical analysis result of this kind. Furthermore, our hope is that the present work will serve as a stepping stone for future studies for more complicated kinetic equations.

**1.1. Multi-scale radiative transfer equation .** We first give a quick overview of the equation. In  $d > 1$  dimension, the equation writes:

$$\partial_t u(t, x, v) = \mathcal{L}u = -\frac{v}{\epsilon} \cdot \nabla_x u(t, x, v) + \frac{\sigma(x)}{\epsilon^2} (\rho(x) - u(t, x, v)), \quad (t, x, v) \in \mathbb{R}^+ \times \Omega_x \times \mathcal{S}^{d-1}, \quad (1)$$

where  $\sigma(x)$  is the scattering cross-section,  $\Omega_x \subset \mathbb{R}^d$ ,  $\epsilon$  is called the Knudsen number, which represents the ratio between the mean free path and the typical domain length, and  $v$  is the angular variable. The density  $\rho$  is defined as follows

$$\rho(x) = \langle u(t, x, v) \rangle_v = \frac{1}{|\mathcal{S}^{d-1}|} \int_{\mathcal{S}^{d-1}} u(t, x, v) dS_v, \quad (2)$$

where  $|\mathcal{S}^{d-1}|$  is the area of  $\mathcal{S}^{d-1}$ , the unit sphere in  $d$  dimensional space, and  $\langle \cdot \rangle_v$  denotes the average with respect to  $v \in \mathcal{S}^{d-1}$ . The equation is written in diffusion scaling, meaning the transport term  $v \cdot \nabla_x u$  and the collision term  $\rho - u$  are multiplied by  $\frac{1}{\epsilon}$  and  $\frac{1}{\epsilon^2}$ , respectively.

Under certain regularity assumption on  $\sigma$ , in the limit of  $\epsilon \rightarrow 0$ , the solution  $u$  of (1) will asymptotically approach  $\rho$  and thus loses its  $v$  dependence. Then the solution of  $\rho$  satisfies the following heat equation (with  $C_d$  being a constant depending on  $d$ ):

$$\partial_t \rho = \nabla_x \cdot \left( \frac{1}{C_d \sigma(x)} \nabla_x \rho \right), \quad (t, x) \in \mathbb{R}^+ \times \Omega_x. \quad (3)$$

This is called the diffusion limit of the radiative transfer equation. This limit is particularly interesting in the present setting as the corresponding solution  $u(t, x, v) \sim \rho(t, x)$ , indicating the solution is essentially of rank 1.

There are two major problems that pose difficulties for numerically solving equation (1). First, a small Knudsen number  $\epsilon \ll 1$ , the regime of interest in this paper, implies that both the transport term and the collision operator are stiff. A standard numerical scheme thus requires time steps that scale with  $\epsilon^2$  and a very fine mesh. Second, equation (1) is posed in an  $2d - 1$  dimensional phase space. Therefore, if the equation is discretized using  $N_x$  points in each spatial direction and  $N_v$  points in each velocity direction, we need to store at least  $N_x^d N_v^{d-1}$  floating point numbers. For  $d = 3$  this is a five-dimensional problem. The large increase in the degrees of freedom for such high-dimensional problems is usually referred to as the *curse of dimensionality* in the literature. Both of these issues contribute to the fact that solving equation (1) is extremely expensive from a computational point of view.

The second problem has been essentially left open. It is a rather widely-accepted fact that the numerical cost depends on the number of grid points (the degrees of freedom) used in the whole domain. However, there has been a large body of work addressing the first problem; namely, can we design a numerical solver that

advances in time with a time-step size decoupled from the stiffness of the equation. A typical solution is to include some form of implicit solver in the numerical treatment in order to enlarge the stability region, and then devise a numerical method that efficiently solves the implicit part of the scheme. This property was later termed *asymptotic-preserving* (AP) in a ground-breaking paper [21], although some earlier schemes exist that were designed to satisfy this property [29]. A systematic investigation of AP was then conducted in a series of works for many (mainly nonlinear) Boltzmann-like equations, see [8, 30, 3, 9, 31, 7]. Also see reviews [20, 23, 10].

**1.2. Dynamical low rank approximation.** Dynamical low rank approximation is a systematic approach to tackle the curse of dimensionality for time-dependent problems. Under the assumption that the solution in fact lives in a low-dimensional manifold, the method looks for the low-rank approximation to the solution at every time step and advances the evolution projected on a low-dimensional tangential space. In particular, for kinetic equations, it is rather straightforward to separate the physical space coordinate and the velocity space:

$$u(t, x, v) = \sum_{i,j=1}^r S_{i,j} X_i(t, x) V_j(t, v), \quad (4)$$

so that the low rank factors  $X_i$  and  $V_j$  depend only on one type of coordinate. Assuming  $r \ll \min(N_x, N_v)$ , this approximation only requires  $O(r(N_x^d + N_v^{d-1}))$  degrees of freedom.

Historically, dynamical low-rank approximations have been considered extensively in quantum mechanics, in which the dimensionality is high. Finding a low rank approximation there makes the computation tractable, see [40, 39] and [33, 34, 4] for a mathematical treatment. The application of the method in a general setting is studied in [26, 27, 37, 1], where the authors study both the matrix case (the approach we will be using here), and a general tensor formats, as is required for very high dimensional problems from quantum mechanics. One significant disadvantage of these algorithm is that they are not robust with respect to over-approximation, i.e. choosing a rank larger than is necessary for the problem at hand. Initially this problem was solved by regularization, and then a major improvement was suggested in [36], in which the so-called *projector splitting integrator* was introduced to make the dynamical low-rank approximation robust with respect to small singular values [25]. This approach was later extended to various tensor formats [34, 35, 19, 38], and it is the approach to be utilized in the present paper.

The application of dynamical low-rank approximation for kinetic equations is relatively recent. Specifically, numerical methods have been proposed for the Vlasov–Poisson [15, 14], the Vlasov–Maxwell [16], and the Boltzmann equation [11]. These are all nonlinear kinetic models and the numerical results are very promising. However, the currently available results all mainly focus on computational aspects and on conserving the physical structure of the underlying equation. A mathematical analysis is lacking.

To analyze the numerical error for a dynamical low-rank algorithm applied to kinetic equations, we have to answer two questions

- (1) Do the solutions have low-rank structures?
- (2) How can we capture the structure dynamically in numerics?

Intuitively, to answer the first question, we utilize the fluid limit obtained on the theoretical level going back to equations (1) and (3). Since one can show that as  $\epsilon \rightarrow 0$  we get  $u(t, x, v) = \rho(t, x)$ , the velocity direction

completely degenerates, and the rank of the representation in equation (4) is simply 1. It is then reasonable to expect that for small  $\epsilon$  the solution is only slightly different from its rank-1 approximation.

To answer the second question, however, requires us to design an appropriate algorithm. As mentioned above, we will use the projector-splitting approach. This leads to a set of three evolution equations for  $S$ ,  $X$ , and  $V$ , respectively. To complete one time step we have to advance all three equations. As will be shown in Section 3, however, the order in which the sub-flows in the splitting are solved is important for preserving the rank. In addition, we will demonstrate that the chosen time integrator plays a crucial role. One can, for example, show that the implicit Euler method, due to the lack of the symmetry, fails to satisfy the correct limit. On the other hand, the Crank–Nicolson method converges to the correct limit and is thus asymptotic preserving.

Before proceeding, let us put the present work in the proper context. There are two basic methods to compute a low-rank approximation of an evolutionary partial differential equations. The first option is to use a so called *projection method* (not to be confused with the projector-splitting integrator for a dynamical low-rank approximation). In this case we first discretize the partial differential equations. We then start with an initial value of fixed rank and compute one time step using the numerical integrator chosen. This, in general, takes us outside of the approximation space (i.e. the rank increases). The so obtained result is then projected back to a manifold of functions with fixed rank. For kinetic equations such an approach was suggested in [28]. The disadvantage of this approach, however, is that an object that does not lie in the approximation space has to be constructed, which implies both a memory as well as a performance penalty. In addition, the derived algorithm is very closely tied to the specific space and time discretization that has been chosen. An alternative is to directly formulate the dynamics of the low-rank approximation by projecting the original equation onto the manifold of functions with a fixed rank. This can be done completely on the continuous level and results in a new set of partial differential equations formulated directly in terms the low-rank factors. As mentioned above, we will follow the latter approach which is usually referred to as a *dynamical low-rank approximation*.

The rest of the paper is organized as follows. In Section 2 we present the numerical method that is applied to the radiative transfer equation. In Section 3 we state and prove the main results. Some parts of the proof in Section 3 are rather tedious. We leave those to the appendix and keep only the core analysis in the main text. Numerical results are then presented in section 4.

## 2. NUMERICAL SCHEME

In this section we follow the framework and notations in [15] and present a numerical method that uses a function of the form given in equation (4) as the approximation space. Our goal is to obtain a low rank approximation to the solution of (1). To define the rank, we first need to equip the spaces with proper measures. For that, we simply use the standard  $L_2$  vector space in both the spatial and the velocity domain. That is, we have

$$\langle f, g \rangle_x = \int f(x)g(x) dx, \quad \langle f, g \rangle_v = \int f(v)g(v) d\mu_v,$$

where  $dx$  is the spatial measure in  $\Omega_x \subset \mathbb{R}^d$ , and  $\mu_v = \frac{1}{|\mathcal{S}^{d-1}|} dv$  is a normalized measure in  $v \in \mathcal{S}^{d-1}$ . Then, any function  $f(x, v)$  that can be expanded by a set of  $r$  orthonormal basis functions in  $x$  and  $v$ , is called rank- $r$ . We collect all these functions together and denote the collection by  $\mathcal{M}$ .

**Definition 1** (Rank- $r$  function in  $L_2(dx dv)$ ). The collection of all rank- $r$  functions is denoted by

$$\mathcal{M} = \{f(x, v) \in L^2(\Omega_x \times \mathcal{S}^{d-1}) : f(x, v) \text{ is rank-}r\},$$

where we call a function  $f(x, v)$  rank- $r$  if there is a set of orthonormal basis functions  $\{X_i, i = 1 \cdots, r\}$  and a set of orthonormal basis functions  $\{V_i, i = 1 \cdots, r\}$  such that

$$f(x, v) = \sum_{i,j=1}^r S_{i,j} X_i(x) V_j(v).$$

Here  $X_i$  are orthonormal in physical space  $x \in \Omega_x$  and  $V_i$  are orthonormal in velocity space  $v \in \mathcal{S}^{d-1}$  with appropriate measures  $dx$  and  $d\mu_v$ , namely

$$\langle X_i, X_j \rangle_x = \int_{\Omega_x} X_i X_j dx = \delta_{ij}, \quad \langle V_i, V_j \rangle_v = \int_{\mathcal{S}^{d-1}} V_i V_j d\mu_v = \delta_{ij}.$$

We note that in this definition, only the rank,  $r$ , is fixed. The basis functions  $X_i$  and  $V_j$  can be arbitrary, as long as the orthogonality condition is satisfied. We further emphasize that  $\mathcal{M}$  is not a function space; it is easily seen that the summation of two rank- $r$  functions may not be rank- $r$ .

It is unlikely that the solution is of rank- $r$ , i.e. in  $\mathcal{M}$ , for all time. However, numerically one can argue that the solution is approximately of low rank. Thus for the numerical solution we seek a rank- $r$  approximation in  $\mathcal{M}$  at every time step. The algorithm is consequently looking for a trajectory on the manifold  $\mathcal{M}$  that resembles the evolution guided by the equation. In some sense, we need to project the equation in  $L^2(\Omega \times \mathcal{S}^{d-1})$  to the manifold and find the equation that governs the dynamics of this trajectory in  $\mathcal{M}$ . Let us denote by  $u(t, x, v)$  the analytic solution and by  $u_r(t, x, v)$  the numerical rank- $r$  approximation. Using the argument above, the governing equation for  $u_r$  is

$$\partial_t u_r = \mathcal{P}_{u_r}(\mathcal{L}u_r) = \mathcal{P}_{u_r} \left( \frac{\sigma(x)}{\epsilon^2} (\rho - u_r) - \frac{v}{\epsilon} \cdot \nabla_x u_r \right), \quad (5)$$

where  $\mathcal{P}_u f$  stands for the projection of  $f$  onto the tangential plane of  $\mathcal{M}$  at  $u$ . This is to ensure that

$$\dot{u}_r \in \mathcal{T}_{u_r} \mathcal{M},$$

where  $\mathcal{T}_{u_r} \mathcal{M}$  denotes the tangential plane of  $\mathcal{M}$  at  $u_r$ . This condition is sufficient to guarantee that  $u_r$  lies in the manifold for all time.

To explicitly express the tangential plane for the manifold  $\mathcal{M}$  and the projection operator, we first notice that at any function  $f \in \mathcal{M}$ , the tangential plane is different and that the form highly depends on  $f$ . Denote

$$f = \sum_{ij} S_{ij} X_i V_j \in \text{Span}\{X_i\}_{i=1}^r \otimes \text{Span}\{V_j\}_{j=1}^r,$$

then the tangential plane is given by

$$\mathcal{T}_f \mathcal{M} = \left\{ g \in L^2(\Omega_x \times \mathcal{S}^{d-1}) : g = \sum_{i,j=1}^r X_i(x) \dot{S}_{i,j} V_j(v) + \dot{X}_i(x) S_{i,j} V_j(v) + X_i(x) S_{i,j} \dot{V}_j(v) \right. \\ \left. \text{with } \dot{S} \in \mathbb{R}^{r \times r}, \dot{X}_i \in L^2(\Omega_x), \dot{V}_j \in L^2(\mathcal{S}^{d-1}), \text{ and } \langle X_i, \dot{X}_j \rangle_x = \langle V_i, \dot{V}_j \rangle_v = 0 \right\}.$$

This set collects all functions whose infinitesimal, when added to  $f$ , still yields a rank- $r$  function. In this definition, we notice that we are allowed to choose arbitrarily an  $r \times r$  matrix  $\dot{S}$ , a function list  $\dot{X}_i$  and a function list  $\dot{V}_i$ , as long as the gauge conditions,  $\langle X_i, \dot{X}_j \rangle_x = \langle V_i, \dot{V}_j \rangle_v = 0$ , are satisfied. We note that the gauge conditions are imposed to guarantee the uniqueness of the low-rank factors. Interested readers are referred to [36] for details.

With this definition, one has:

- If  $g \in \mathcal{T}_f \mathcal{M}$ , the orthogonality and gauge condition quickly allows us to write

$$\dot{S}_{ij} = \langle X_i V_j, g \rangle_{x,v}, \quad \dot{X}_i = \langle X_i, g \rangle_x, \quad \dot{V}_i = \langle V_i, g \rangle_v,$$

- if  $g \notin \mathcal{T}_f \mathcal{M}$ , its projection onto  $\mathcal{T}_f \mathcal{M}$  can also be easily formulated as follows

$$\mathcal{P}_f g = \mathcal{P}_X g + \mathcal{P}_V g - \mathcal{P}_V \mathcal{P}_X g, \quad \forall g \in L^2(\Omega_x \times \mathcal{S}^{d-1}), \quad (6)$$

where the spatial and velocity projection are

$$\mathcal{P}_X g = \sum_i^r \langle X_i, g \rangle_x X_i, \quad \mathcal{P}_V g = \sum_i^r \langle V_i, g \rangle_v V_i, \quad \text{and} \quad \mathcal{P}_V \mathcal{P}_X g = \sum_{i,j}^r X_i \langle X_i V_j, g \rangle_{x,v} V_j.$$

Inserting (6) into (5) gives us the governing equation for  $u_r$ :

$$\partial_t u_r = \mathcal{P}_{u_r}(\mathcal{L} u_r) = (\mathcal{P}_{X_{u_r}} + \mathcal{P}_{V_{u_r}} - \mathcal{P}_{V_{u_r}} \mathcal{P}_{X_{u_r}})(\mathcal{L} u_r). \quad (7)$$

The numerical method will then be developed upon this formulation. We discuss the semi-discrete (in time) and the fully-discrete schemes in details in the following subsections. This will give us a formulation for one time step. To devise an asymptotic preserving scheme for integrating from  $t = 0$  to the final time  $t_{\max}$  we need a thorough understanding of the error analysis. In fact, the implicit Euler and Crank-Nicolson behave slightly different. To optimally suit our purpose we run the Euler for one step before shifting to Crank-Nicolson scheme. We defer a detailed discussion to the end of Section 3.

**Remark 1.** We wrap up this introduction with a comment on rank- $r$  approximations. In fact, all numerical methods to solve PDEs are rank- $r$  approximations. Let us suppose we have a numerical method with  $N$  grid points in both  $x$  and  $v$ . Then

$$u(x_m, v_n) \approx \sum_{i,j=1}^N u_{ij} \Phi_i(x_m) \Phi_j(v_n),$$

where  $\Phi_i$  are basis functions we use to approximate the solution. For example, in a finite difference method we set  $\Phi_i(x_m) = \delta_i(x_m) = \delta_{im}$  as the Kronecker delta function or hat functions that peak at  $x_i$  (similar argument holds for  $\Phi_i(v_n)$ ) and  $u_{ij}$  is the numerical solution evaluated at  $x_i$  and  $v_j$ . To find a numerical solution on this mesh is equivalent to finding a rank- $N$  approximation with fixed  $X_i$  and  $V_j$ . Then  $u_{ij}$  plays the role of  $S_{ij}$  above. This is typically not formulated in this way as the rank  $r = N$  is very large. When we consider a low-rank approximation, as in this paper, we will always assume that  $r \ll N$ . To achieve this, the functions  $X_i$  and  $V_j$  need to evolve in time according to the dynamics of the equation.

**2.1. Semi-discrete low rank splitting method.** In this section, we develop a projector-splitting method to solve equation (7). In order to be concise, we simply denote the low rank solution  $u_r$  by  $u$  and we decompose

the solution using its low-rank representation:

$$u(t, x, v) = \sum_{i,j=1}^r X_i(t, x) S_{i,j}(t) V_j(t, v) = \mathbf{X}(t, x) \mathbf{S}(t) \mathbf{V}^\top(t, v) = \mathbf{X}(t, x) \mathbf{L}(t, v) = \mathbf{K}(t, x) \mathbf{V}^\top(t, v) \quad (8)$$

where  $\mathbf{X}$  and  $\mathbf{V}$  collects the basis functions

$$\mathbf{X}(t, x) = [X_1(t, x), X_2(t, x), \dots, X_r(t, x)] , \quad \text{and} \quad \mathbf{V}(t, v) = [V_1(t, v), V_2(t, v), \dots, V_r(t, v)] .$$

This formulation will also be quite useful later when we introduce a space discretization. We will also be using quantities  $\mathbf{K}$  and  $\mathbf{L}$ :

$$\mathbf{L}(t, v) = \mathbf{S}(t) \mathbf{V}^\top(t, v) = [L_1(t, v), L_2(t, v), \dots, L_r(t, v)]^\top , \quad (9)$$

$$\mathbf{K}(t, x) = \mathbf{X}(t, x) \mathbf{S}(t) = [K_1(t, x), K_2(t, x), \dots, K_r(t, x)] . \quad (10)$$

Computing (7) at discrete times  $t_n$  amounts to finding the governing equations that provide the updates of

$$\mathbf{X}^n , \quad \mathbf{V}^n , \quad \text{and} \quad \mathbf{S}^n ,$$

respectively, for all  $t_n$  with  $n \geq 1$ .

To specify the initial data into the format, we project the initial condition onto  $\mathcal{M}$  using the singular value decomposition (SVD):

$$u(t=0, x, v) \approx \sum_{i,j=1}^r X_i(t=0, x) S_{i,j}(t=0) V_j(t=0, v) = \mathbf{X}^0(x) \mathbf{S}^0 \mathbf{V}^0(v) . \quad (11)$$

For updating  $\mathbf{X}, \mathbf{V}, \mathbf{S}$ , the Lie-Trotter splitting is used. From time step  $t_n$  to  $t_{n+1} = t_n + \Delta t$ , we split the three operators on the right hand side of (7) into three sub-steps, namely

$$\partial_t u = \mathcal{P}_{\mathbf{X}_u} \left( \frac{\sigma(x)}{\epsilon^2} (\rho - u) - \frac{v}{\epsilon} \cdot \nabla_x u \right) , \quad (12)$$

$$\partial_t u = -\mathcal{P}_{\mathbf{V}_u} \mathcal{P}_{\mathbf{X}_u} \left( \frac{\sigma(x)}{\epsilon^2} (\rho - u) - \frac{v}{\epsilon} \cdot \nabla_x u \right) , \quad (13)$$

$$\partial_t u = \mathcal{P}_{\mathbf{V}_u} \left( \frac{\sigma(x)}{\epsilon^2} (\rho - u) - \frac{v}{\epsilon} \cdot \nabla_x u \right) . \quad (14)$$

This splitting (12)-(14) takes place for each time step. That is, given the numerical solution at time  $t_n$  we update the solution to  $t_{n+1}$  by solving the three equations one after another. All equations are advanced for a full time step  $\Delta t$ . Different from directly solving (7), each sub-step only changes one part of the decomposition. In particular, the first splitting step (12) preserves  $\mathbf{X}$ , the last (14) preserves  $\mathbf{V}$ , and the middle step (13) merely updates  $\mathbf{S}$ . This allows us to update the three components separately without disturbing others. Below we detail the evolution of each sub-step:

- Updating (12):

Starting with  $u^n(x, v) = \mathbf{X}^n(x) \mathbf{S}^n(\mathbf{V}^n(v))^\top$ , in this sub-step, we run (12) for a full time step  $\Delta t$ , and we denote the result by  $u^{n+1/3}(x, v)$ . Since the step preserves  $\mathbf{X}$ :

$$\mathbf{X}^{n+1/3}(x) = \mathbf{X}^n(x) .$$

To update  $S^{n+1/3}$  and  $V^{n+1/3}(v)$ , we plug the low rank formulation (8) into (12) and obtain

$$\partial_t L_i(t, v) + \frac{1}{\epsilon} \sum_{j=1}^r \langle X_i^n, v \cdot \nabla X_j^n \rangle_x L_j(t, v) = \frac{1}{\epsilon^2} \sum_{j=1}^r \langle X_i^n, \sigma(x) X_j^n \rangle_x (\langle L_j \rangle_v - L_j(t, v)), \quad (15)$$

with  $1 \leq i \leq r$ . By using equation (9) we can simplify (15) to

$$\partial_t L(t, v) + \frac{1}{\epsilon} \sum_{k=1}^d v_k A_{\partial_k}^n L(t, v) = \frac{1}{\epsilon^2} A_\sigma^n (\langle L(t, \cdot) \rangle_v - L(t, v)), \quad (16)$$

where  $v = [v_1, \dots, v_d]$ , and  $A_{\partial_k}^n$  and  $A_\sigma^n$ , both  $\in \mathbb{R}^{r \times r}$ , are matrix versions of the differential operator and the scattering operator respectively:

$$[A_{\partial_k}^n]_{i,j} = \langle X_i^n(\cdot), \partial_k X_j^n(\cdot) \rangle_x, \quad (1 \leq k \leq d), \quad \text{and} \quad [A_\sigma^n]_{i,j} = \langle X_i^n(\cdot), \sigma(\cdot) X_j^n(\cdot) \rangle_x. \quad (17)$$

We denote the solution to (16) by  $L^{n+1/3}(v)$ , and  $S^{n+1/3}$  and  $V^{n+1/3}(v)$  are obtained through the Gram-Schmidt process (QR factorization) which ensures the orthogonality of  $V^{n+1/3}(v)$ :

$$L^{n+1/3}(v) = S^{n+1/3} \left( V^{n+1/3}(v) \right)^\top, \quad \text{and} \quad u^{n+1/3} = (X S V^\top)^{n+1/3}.$$

- Updating (13):

In this step, equation (13) is ran for a full time step  $\Delta t$  with initial condition  $u^{n+1/3}$ . We denote the result by  $u^{n+2/3}$ . Since the step only changes  $S$ , we immediately obtain

$$X^{n+2/3}(x) = X^{n+1/3}(x), \quad \text{and} \quad V^{n+2/3}(v) = V^{n+1/3}(v).$$

Plugging the low rank representation (8) into (13), we obtain, for  $1 \leq i, j \leq r$ ,

$$\begin{aligned} \partial_t S_{i,j}(t) - \frac{1}{\epsilon} \sum_{p,q=1}^r \left\langle X_i^n V_j^{n+2/3}, (v \cdot \nabla_x X_p^n) V_q^{n+2/3} \right\rangle_{x,v} S_{p,q}(t) \\ = - \frac{1}{\epsilon^2} \sum_{p,q=1}^r \langle X_i^n, \sigma(x) X_p^n \rangle_x S_{p,q}(t) \left( \langle V_j^{n+2/3} \rangle_v \langle V_q^{n+2/3} \rangle_v - \delta_{j,q} \right). \end{aligned}$$

In matrix form this can be written as

$$\partial_t S(t) - \frac{1}{\epsilon} \sum_{k=1}^d A_{\partial_k}^n S(t) \Xi_{v_k}^{n+2/3} = - \frac{1}{\epsilon^2} A_\sigma^n S(t) \Gamma^{n+2/3}, \quad (18)$$

where  $\Xi_{v_k}$  and  $\Gamma$ , both  $\in \mathbb{R}^{r \times r}$ , are the matrix versions of the multiplication operator associated to  $v_k$  ( $1 \leq k \leq d$ ) and the density term, respectively:

$$[\Xi_{v_k}]_{i,j} = \langle V_i(\cdot), (\cdot)_k V_j(\cdot) \rangle_v, \quad \text{and} \quad [\Gamma]_{i,j} = \langle V_i(\cdot) \rangle_v \langle V_j(\cdot) \rangle_v - \delta_{i,j}. \quad (19)$$

We denote the computed update of (18) by  $S^{n+2/3}$ .

- Updating (14):

In this step, (14) is ran for a full time step  $\Delta t$  with initial value  $u^{n+2/3}$ . We denote the result by  $u^{n+1}$ . This step preserves  $V$ . Thus,

$$V^{n+1}(v) = V^{n+2/3}(v).$$

To update  $X^{n+1}$  and  $S^{n+1}$ , the low rank formulation (8) is plugging into (12). Then for all  $1 \leq j \leq r$  we have

$$\partial_t K_j(x, t) + \frac{1}{\epsilon} \sum_{i=1}^r \langle V_j^{n+1}, (v \cdot \nabla_x K_i) V_i^{n+1} \rangle_v = \frac{1}{\epsilon^2} \sum_{i=1}^r K_i(x, t) (\langle V_i^{n+1} \rangle_v \langle V_j^{n+1} \rangle_v - \delta_{i,j}),$$

This can be written in matrix form as follows

$$\partial_t K(t, x) + \frac{1}{\epsilon} \sum_{k=1}^d \partial_k K(t, x) \Xi_{v_k}^{n+1} = \frac{1}{\epsilon^2} K(t, x) \Gamma^{n+1}, \quad (20)$$

with (since  $V^{n+2/3} = V^{n+1}$ )

$$\Xi^{n+1} = \Xi^{n+2/3}, \quad \text{and} \quad \Gamma^{n+1} = \Gamma^{n+2/3}.$$

Solving this equation we obtain  $K^{n+1}(v)$ , and the orthogonality of  $X^{n+1}$  is ensured through the Gram-Schmidt process:

$$K^{n+1}(x) = X^{n+1}(x) S^{n+1}.$$

With these three steps completed, one finally arrives at numerical solution at time  $t_{n+1}$

$$u^{n+1} = X^{n+1}(x) S^{n+1} (V^{n+1}(v))^\top.$$

**2.2. Fully-discrete low rank splitting method.** The beforementioned method will now be discretized. Due to the stiffness of the equations, an implicit scheme will be applied. We denote

$$\mathcal{X} = \{x_1, x_2, \dots, x_{N_x}\}, \quad \mathcal{V} = \{v_1, v_2, \dots, v_{N_v}\}$$

the sets of discrete points in  $\Omega_x$  and  $S^{d-1}$ . The discrete solution can then be represented as follows

$$\mathbb{R}^{N_x \times N_v} \ni u^n = X^n S^n (V^n)^\top,$$

where  $S^n = S^n$  and

$$X^n = [X_1^n \ X_2^n \ \dots \ X_r^n] \in \mathbb{R}^{N_x \times r}, \quad \text{and} \quad V^n = [V_1^n \ V_2^n \ \dots \ V_r^n] \in \mathbb{R}^{N_v \times r}, \quad (21)$$

with  $X_i^n$  and  $V_i^n$  denote the  $i$ -th mode evaluated at the discrete points in  $\mathcal{X}$  and  $\mathcal{V}$ .

We now discuss the implicit time integration of the three equations (16), (18), and (20). The asymptotic analysis will be performed based on this fully-discrete formulation.

- For updating (16),  $X$  is preserved and thus  $X^{n+1/3} = X^n$ . The direct application of the implicit Euler scheme gives

$$\begin{cases} \frac{L^{n+1/3} - L^n}{\Delta t} + \frac{1}{\epsilon} \sum_{k=1}^d A_{\partial_k}^n L^{n+1/3} \Pi_{v_k} = \frac{A_\sigma^n}{\epsilon^2} L^{n+1/3} C, \\ \text{QR decomposition: } L^{n+1/3} = S^{n+1/3} (V^{n+1})^\top \end{cases}, \quad (22)$$

and if Crank–Nicolson is used, the scheme is written as

$$\begin{cases} \frac{\mathbf{L}^{n+1/3} - \mathbf{L}^n}{\Delta t} + \frac{1}{\epsilon} \sum_{k=1}^d \mathbf{A}_{\partial_k}^n \left( \frac{\mathbf{L}^{n+1/3} + \mathbf{L}^n}{2} \right) \Pi_{v_k} = \frac{\mathbf{A}_\sigma^n}{\epsilon^2} \frac{\mathbf{L}^{n+1/3} + \mathbf{L}^n}{2} \mathbf{C} \\ \text{QR decomposition: } \mathbf{L}^{n+1/3} = \mathbf{S}^{n+1/3} (\mathbf{V}^{n+1/3})^\top \end{cases} \quad (23)$$

We have used

$$\mathbf{A}_{\partial_k}^n = (\mathbf{X}^n)^\top \mathbf{D}_k \mathbf{X}^n, \quad \Pi_{v_k} = \text{diag}(\mathcal{V}_k), \quad \mathbf{A}_\sigma^n = \mathbf{X}^\top \Sigma \mathbf{X}, \quad \text{and} \quad \mathbf{C} = \frac{1}{N_v} e e^\top - \mathbf{I}_{N_v}, \quad (24)$$

with  $e = (1, 1, \dots, 1)^\top$ .  $\Sigma = \text{diag}(\sigma(\mathcal{X}))$  is an  $N_x \times N_x$  matrix with evaluations of  $\sigma$  at the grid points in  $\mathcal{X}$  assigned as diagonal entries and  $\mathbf{D}_k$  is the discrete approximation of  $\partial_{x_k}$ . The specific form of  $\mathbf{D}_k$  depends on the spatial discretization. We have used the simple rectangle rule for the integration in  $\mu_v$ . This determines the form of  $\mathbf{C}$ . Other numerical integral rules could also be applied and the specific form of  $\mathbf{C}$  will change accordingly. Obviously  $\mathbf{A}_{\partial_k}^n$  and  $\mathbf{A}_\sigma^n$  are the discrete versions of (17).

– For updating (18), we note that  $\mathbf{X}$  and  $\mathbf{V}$  are preserved in this step. That is,

$$\mathbf{X}^{n+2/3} = \mathbf{X}^{n+1/3}, \quad \text{and} \quad \mathbf{V}^{n+2/3} = \mathbf{V}^{n+1/3}.$$

The direct application of the implicit Euler scheme gives

$$\frac{\mathbf{S}^{n+2/3} - \mathbf{S}^{n+1/3}}{\Delta t} - \frac{1}{\epsilon} \sum_{k=1}^d \mathbf{A}_{\partial_k}^n \mathbf{S}^{n+2/3} \Xi_{v_k}^{n+2/3} = -\frac{\mathbf{A}_\sigma^n}{\epsilon^2} \mathbf{S}^{n+2/3} \Gamma^{n+2/3}. \quad (25)$$

Similarly, if Crank–Nicolson is used, the scheme can be written as

$$\frac{\mathbf{S}^{n+2/3} - \mathbf{S}^{n+1/3}}{\Delta t} - \frac{1}{\epsilon} \sum_{k=1}^d \mathbf{A}_{\partial_k}^n \frac{\mathbf{S}^{n+2/3} + \mathbf{S}^{n+1/3}}{2} \Xi_{v_k}^{n+2/3} = -\frac{\mathbf{A}_\sigma^n}{\epsilon^2} \frac{\mathbf{S}^{n+2/3} + \mathbf{S}^{n+1/3}}{2} \Gamma^{n+2/3}. \quad (26)$$

Here  $\Xi_{v_k}^{n+2/3}$  and  $\Gamma^{n+2/3}$ , both  $r \times r$ , are discrete versions of (19), defined by

$$\Xi_{v_k}^{n+2/3} = (\mathbf{V}^{n+2/3})^\top \Pi_{v_k} \mathbf{V}^{n+2/3}, \quad \text{and} \quad \Gamma^{n+2/3} = (\mathbf{V}^{n+2/3})^\top \mathbf{C} \mathbf{V}^{n+2/3}. \quad (27)$$

– Finally for updating (16), we note  $\mathbf{V}^{n+1} = \mathbf{V}^{n+2/3}$ ,  $\Gamma^{n+1} = \Gamma^{n+2/3}$ ,  $\Xi^{n+1} = \Xi^{n+2/3}$  are preserved. Defining

$$\mathbf{K}^{n+2/3} = \mathbf{X}^{n+2/3} \mathbf{S}^{n+2/3}, \quad (28)$$

and applying the implicit Euler method we obtain

$$\begin{cases} \frac{\mathbf{K}^{n+1} - \mathbf{K}^{n+2/3}}{\Delta t} + \frac{1}{\epsilon} \sum_{k=1}^d \mathbf{D}_k \mathbf{K}^{n+1} \Xi_{v_k}^{n+1} = \frac{\Sigma}{\epsilon^2} \mathbf{K}^{n+1} \Gamma^{n+1} \\ \text{QR decomposition: } \mathbf{X}^{n+1} \mathbf{S}^{n+1} = \mathbf{K}^{n+1} \end{cases} \quad (29)$$

where we used the same definition of  $\Sigma = \text{diag}(\sigma(\mathcal{X}))$ . Crank–Nicolson method will not be used in the last step and thus we do not specify it.

We finalize the update for

$$u^{n+1} = \mathbf{X}^{n+1} \mathbf{S}^{n+1} (\mathbf{V}^{n+1})^\top.$$

### 3. PROPERTIES OF THE NUMERICAL SCHEME

We investigate the properties of the numerical method in this section. In particular we will discuss the computational complexity and prove the method preserves the asymptotic limit in the strong collisional regime.

**3.1. Computational complexity.** To analyze the computational complexity is rather straightforward. Denote  $r$  the rank,  $N_x$  and  $N_v$  the number of grid points in physical space  $x$  and velocity space  $v$  respectively. The matrices in the updating formula,  $\mathbf{X}^n$ ,  $\mathbf{S}^n$ ,  $\mathbf{V}^n$  are computed by solving (22), (25), (29). The following cost incurs:

- Preparation: Calculation of  $\mathbf{A}_{\partial_k}^n, \mathbf{A}_\sigma^n$  needs  $O(r^2 N_x^2)$  floating point operations (flops).
- Update V: Calculation of  $\mathbf{L}^n$  needs  $O(r^3 N_v)$  flops.  
 Calculation of  $\Pi_{v_k} \otimes \mathbf{A}_{\partial_k}^n, \mathbf{C} \otimes \mathbf{A}_\sigma^n$  need  $O(r^2 N_v)$  flops.  
 Solving  $\mathbf{L}^{n+1}$  needs  $O(r^3 N_v^3)$  flops.  
 Using QR decomposition to obtain  $\mathbf{S}^{n+1/3}, \mathbf{V}^{n+1/3}$  needs  $O(N_v^3)$ .
- Update S: Calculation of  $\Xi_{v_k}^{n+2/3}$  and  $\Gamma^{n+2/3}$  needs  $O(r^2 N_v^2)$   
 Calculation of  $\Xi_{v_k}^{n+2/3} \otimes \mathbf{A}_{\partial_k}^n, \Gamma^{n+2/3} \otimes \mathbf{A}_\sigma^n$  needs  $O(r^3)$  flops.  
 Solving  $\mathbf{S}^{n+2/3}$  needs  $O(r^6)$  flops.
- Update X: Calculation of  $\mathbf{K}^{n+2/3}$  needs  $O(r^3 N_x)$  flops.  
 Calculation of  $\Xi_{v_k}^{n+2/3} \otimes \mathbf{D}_k, \Gamma^{n+2/3} \otimes \Sigma$  needs  $O(r^2 N_x)$  flops.  
 Solving  $\mathbf{K}^{n+1}$  needs  $O(r^3 N_x^3)$  flops.  
 Using QR decomposition to obtain  $\mathbf{X}^{n+1}, \mathbf{S}^{n+1}$  needs  $O(N_x^3)$ .

Because  $r = O(1) \ll N_x, N_v$ , in conclusion, we need  $O(N_x^3 + N_v^3)$  flops per time step, instead of the  $O(N_x^3 N_v^3)$ .

**3.2. Intuition of the error analysis.** Before describing and proving our results in detail, in this section we first give a relatively vague justification on why the method works. As described in the introduction, there are two points we need to make:

- Why the true solution has an approximate low rank structure? This question is a rather fundamental, and is independent of the method chosen: the rank structure of the solution purely depends on the governing PDE we are studying here.
- Why the method keeps track of the low rank structure? This question concerns the behavior of the specific method (dynamic low-rank approximation) we choose to use here.

The two questions will be addressed respectively in the following two subsections.

**3.2.1. Foundation: the low rank structure in the solution.** To justify the low rank structure of the linearized Boltzmann equation, we simply will cite the following result [2]

**Theorem 1** (Theorem 2 of [2]). *Denote  $u$  the solution to the linear Boltzmann equation*

$$\partial_t u^\epsilon = \mathcal{L}u^\epsilon = \frac{\sigma}{\epsilon^2} \mathcal{L}_0 u^\epsilon + \frac{1}{\epsilon} \mathcal{L}_1 u^\epsilon, \quad (t, x, v) \in \mathbb{R}^+ \times \Omega_x \times \mathcal{S}^{d-1}, \quad (30)$$

where  $\mathcal{L}_0 u = \rho - u$  and  $\mathcal{L}_1 u = -v \cdot \nabla_x u$ . Then in the zero limit of  $\epsilon$ , the solution converges to the solution of the diffusion equation:

$$\partial_t \rho = \nabla_x \cdot \left( \frac{1}{d\sigma} \nabla_x \rho \right), \quad (t, x) \in \mathbb{R}^+ \times \Omega_x,$$

in the sense that

$$\|u^\epsilon(t, x, v) - \rho(t, x)\|_{L_2(dx d\mu)} \leq O(\epsilon).$$

We note that periodic boundary conditions are imposed in the original theorem to avoid complications that may come from the boundary layers. Essentially this theorem states that in the zero limit of  $\epsilon$ ,  $u(t, x, v)$  loses its velocity dependence, and the dynamics will purely be reflected in the physical space. In some sense:

$$u(t, x, v) = \rho(x) + \mathcal{O}(\epsilon),$$

can be seen as the rank-1 approximation with the threshold set at any value bigger than  $\epsilon$ .

The proof for the theorem follows the Hilbert expansion. Formally, writing  $u = u_0 + \epsilon u_1 + \epsilon^2 u_2 + \dots$ , we plug it back in the original equation and get:

$$\begin{aligned} \mathcal{O}\left(\frac{1}{\epsilon^2}\right): \quad \mathcal{L}_0 u_0 &= \langle u_0 \rangle_v - u_0 = 0, \quad \Rightarrow \quad u_0(t, x, v) = u_0(t, x), \\ \mathcal{O}\left(\frac{1}{\epsilon}\right): \quad \mathcal{L}_0 u_1 &= \langle u_1 \rangle_v - u_1 = v \cdot \nabla_x u_0, \quad \Rightarrow \quad u_1(t, x, v) = -v \cdot \nabla_x u_0(t, x), \\ \mathcal{O}(1): \quad \partial_t u_0 &= \mathcal{L}_1 u_1 + \mathcal{L}_0 u_2, \quad \Rightarrow \quad \partial_t u_0 = \langle (-v \cdot \nabla_x)^2 \rangle_v u_0, \end{aligned} \quad (31)$$

in which the last equation gives us the diffusion limit. As seen in the expansion, the essence of the proof mainly lies in showing that

$$u_0 \in \text{Null} \mathcal{L}_0,$$

and then tracing the dynamics of  $u_0$  in the null space. Showing Theorem 1 rigorously then amounts to bounding  $u_2$  uniformly in  $\epsilon$ , and we omit it from here.

**3.2.2. Capture the structure along the dynamics.** It is not straightforward to show that the dynamical low-rank approximation method captures the rank structure of the solution. In fact, the direct calculation would suggest otherwise: recall the dynamic low-rank approximation solution governed by the following equation

$$\partial_t u_r = \mathcal{P}_{u_r} \mathcal{L} u_r = \mathcal{P}_{u_r} \left[ \frac{1}{\epsilon^2} \mathcal{L}_0 u_r + \frac{1}{\epsilon} \mathcal{L}_1 u_r \right], \quad (32)$$

and compare it with the original one (30), it is rather easy to see that one essentially need to show that

$$(\mathcal{I} - \mathcal{P}_{u_r}) \mathcal{L} u = (\mathcal{I} - \mathcal{P}_X)(\mathcal{I} - \mathcal{P}_V) \mathcal{L} u \ll \mathcal{O}(1)$$

in some norm, where  $X$  and  $V$  are basis functions of  $u_r$ . This does not seem to be an easy task. On the contrary, concerning that  $\mathcal{L} u$  contains stiff terms such as  $\frac{\rho - u}{\epsilon^2}$ , a brute-force calculation would suggest that the error is of order  $1/\epsilon \gg \mathcal{O}(1)$ .

This straightforward approach, however, overlooks the information hidden in the equation. To show the method keeps  $u_r - u$  small along the evolution, some delicacy from the equation needs to be employed. As will be presented in further details in Section 3.3, the proof largely relies on the separation of scales and one needs

to perform the order by order matching of the scales to derive a clearer view of the solution structure. For that we perform the same analysis as done in (31), and asymptotically expand  $u_r = u_{r,0} + \epsilon u_{r,1} + \dots$ . Plugging it back into equation (32), one has, in the leading order:

$$\mathcal{O}\left(\frac{1}{\epsilon^2}\right): \quad \mathcal{P}_{u_r} \mathcal{L}_0 u_{r,0} = 0.$$

Noting that from the definition of  $\mathcal{L}_0$ ,

$$\text{if } u_r \in \text{Span}\{X_i\} \otimes \text{Span}\{V_j\} \quad \text{then} \quad \mathcal{L}_0 u_r = \rho - u_r = \langle u_r \rangle_v - u_r \in \text{Span}\{X_i\} \otimes \text{Span}\{V_j\},$$

thus

$$\mathcal{P}_{u_r} \mathcal{L}_0 u_{r,0} = \mathcal{L}_0 u_{r,0} = 0.$$

which further suggests that the leading order of the numerical solution

$$u_{r,0} \in \text{Null} \mathcal{L}_0.$$

This at least implies the reduced order equation (32) has its leading order lying in the correct space. Whether it preserves the correct equilibrium state is up to more delicate derivations in the higher order expansions, and thus is left to the following section, where we directly tackle the problem in the fully discrete setting, and show that the numerical scheme indeed captures the diffusion phenomenon.

**3.3. Asymptotic preserving.** Following the intuition from the previous section, we give the rigorous proof that shows that the method captures the diffusion limit in the  $\epsilon \rightarrow 0$  limit.

It is a rather challenging task to design a numerical method for a stiff equation with the discretization being independent of the smallest scale. For an equation with small  $\epsilon$  dependence, usually the solution shows variations at fine scale, and in order to preserve these variations, the discretization has to be small, leading to a large number of degrees of freedom, driving up the numerical cost. If a method has its discretization relaxed from requirements at the finest scale, while still preserves the asymptotic  $\epsilon \rightarrow 0$  limit of the equation, we call it an asymptotic preserving (AP) method. It is an attractive property for a numerical method to have.

In this section, we will prove that in our method, by injecting the low-rank structure into numerical solutions, one can automatically capture the diffusion limit (3), with  $\Delta t$ ,  $\Delta x$ ,  $\Delta v$  and  $r$  all independent of  $\epsilon$ , and thus is an AP method. Furthermore,  $r$  can be as small as 1. We note that the analysis for Crank-Nicolson and implicit Euler shares some similarities but Crank-Nicolson enjoys a symmetry that allows us to pass to the asymptotic limit.

**3.3.1. Asymptotic analysis of the implicit Euler method.** To unify the notation, throughout this section, we denote  $u^n$  a matrix of size  $N_x N_v$  with  $u_{ij}^n$  being the numerical solution at  $t_n, x_i, v_j$ . Denote  $e = [1, \dots, 1]^\top$  a column vector of length  $N_v$ , then  $\rho^n = u^n e$  is a vector of length  $N_x$  representing the discrete version of  $\rho$  at time  $t_n$  for spatial grid points  $\mathcal{X}$ . The hope is to show that density  $\rho^n$  solves equation (3) in the limit  $\epsilon \rightarrow 0$ .

Our first result concerns the behavior of the implicit Euler method in the limit  $\epsilon \rightarrow 0$ .

**Theorem 2.** *We employ the implicit Euler method to compute  $u^{n+1}$  from  $u^n$ , using equations (22), (25) and (29). Denote*

$$u = u_0 + \epsilon u_1 + \dots, \quad \text{and} \quad \rho = \rho_0 + \epsilon \rho_1 + \dots,$$

then, under some mild conditions (see Assumption 1 in Appendix), we have

$$\|\rho^{n+2/3} - \rho^n\|_2 = O\left(\frac{(\Delta t)^2}{(\Delta x)^2}\right) + O(\epsilon), \quad (33)$$

and

$$\frac{\rho_0^{n+1} - \rho_0^{n+2/3}}{\Delta t} = \frac{1}{d} \sum_{k=1}^d \mathbf{D}_k (\Sigma^{-1} \mathbf{D}_k \rho_0^{n+1}). \quad (34)$$

Furthermore,

$$u^{n+1} = \rho_0^{n+1} e^\top + O(\epsilon),$$

This means in the  $\epsilon \rightarrow 0$  limit, the numerical solution is approximately rank 1, with the density solving the diffusion equation with implicit Euler method.

**Remark 2. The bad.** We note that the implicit low-rank integrator based on the implicit Euler scheme is only asymptotic preserving if the time step size  $\Delta t$  is chosen extremely small, due to the  $O((\Delta t)^2/(\Delta x)^2)$  error term. For example, even if we choose  $\Delta t \propto (\Delta x)^2$  the error is only  $O(\Delta t)$  and we end up with a global error of order  $O(1)$ . This renders this numerical method impractical for time integration.

**Remark 3. The good.** The method is able to capture the correct low-rank structure. This can be easily seen from the result as for  $\epsilon \rightarrow 0$  we have  $u^{n+1} = \rho_0^{n+1} e^\top$ . Thus, the solution has rank 1 and is constant in  $v$ , which is precisely the analytic result derived for the diffusion limit, shown in Theorem 1.

*Proof.* The main ingredient in the proof is an asymptotic expansion in  $\epsilon$  and analyzing matrix properties. Throughout the proof, all quantities of interests will be expanded using the following ansatz

$$p = p_0 + \epsilon p_1 + \epsilon^2 p_2 + \dots \quad (35)$$

We now proceed by performing the three steps in the low-rank projector splitting integrator.

**Step 1:** This step preserves  $\mathbf{X}$  and updates  $\mathbf{L}$ . Thus, we plug the asymptotic expansion of  $\mathbf{L}$  into equation (22) and obtain

$$\begin{cases} O(1/\epsilon): & \mathbf{A}_\sigma^n \mathbf{L}_0^{n+1/3} \mathbf{C} = 0 \\ O(1): & \sum_{k=1}^d \mathbf{A}_{\partial_k}^n \mathbf{L}_0^{n+1/3} \Pi_{v_k} = \mathbf{A}_\sigma^n \mathbf{L}_1^{n+1/3} \mathbf{C} \\ O(\epsilon): & \frac{\mathbf{L}_0^{n+1/3} - \mathbf{L}_0^n}{\Delta t} + \sum_{k=1}^d \mathbf{A}_{\partial_k}^n \mathbf{L}_1^{n+1/3} \Pi_{v_k} = \mathbf{A}_\sigma^n \mathbf{L}_2^{n+1/3} \mathbf{C} \end{cases} \quad (36)$$

Since  $\mathbf{A}_\sigma^n$  is invertible, the equation for the leading order implies that  $\mathbf{L}_0^{n+1/3}$  lies in the null space of  $\mathbf{C}^\top$ . According to equation (24)  $\mathbf{C}$  is symmetric with null space  $\text{span}\{e\}$ . Thus, we have at once

$$\mathbf{L}_0^{n+1/3} = l_0^{n+1/3} e^\top, \quad (37)$$

where the  $r \times 1$  vector  $l_0^{n+1/3}$  is yet to be determined. To find  $l_0^{n+1/3}$  we first solve the  $O(1)$  equation for  $\mathbf{L}_1^{n+1/3}$

$$\mathbf{L}_1^{n+1/3} = - \sum_{k=1}^d (\mathbf{A}_\sigma^n)^{-1} \mathbf{A}_{\partial_k}^n l_0^{n+1/3} e^\top \Pi_{v_k} + l_1^{n+1/3} e^\top. \quad (38)$$

The term  $l_1^{n+1/3} e^\top$  gives the contribution of  $\mathbf{L}_1^{n+1/3}$  that lies in the null space of  $\mathbf{C}$ . Thus, the vector  $l_1^{n+1/3} \in \mathbb{R}^{r \times 1}$  is not yet determined by the previous equation. We now close the system by considering the  $O(\epsilon)$  order.

Multiplying  $e$  on both sides yields

$$\frac{\mathbf{L}_0^{n+1/3}e - \mathbf{L}_0^n e}{\Delta t} + \sum_{k=1}^d \mathbf{A}_{\partial_k}^n \mathbf{L}_1^{n+1/3} \Pi_{v_k} e = 0.$$

Plugging (38) into this equation and using

$$e^\top \Pi_{v_{k_1}} \Pi_{v_{k_2}} e = \frac{N_v}{d} \delta_{k_1, k_2}, \quad e^\top \Pi_{v_k} e = 0,$$

we obtain

$$\frac{l_0^{n+1/3} - \mathbf{L}_0^n e / N_v}{\Delta t} + \frac{1}{d} \sum_{k=1}^d \mathbf{A}_{\partial_k}^n (\mathbf{A}_\sigma^n)^{-1} \mathbf{A}_{\partial_k}^n l_0^{n+1/3} = 0.$$

Thus, we have closed the system for updating  $l_0^{n+1/3}$ . Since  $u_0^{n+1/3} = \mathbf{X}^n \mathbf{L}_0^{n+1/3} = \mathbf{X}^n l_0^{n+1/3} e^\top$  and  $\rho^{n+1/3} = u_0^{n+1/3} e = \mathbf{X}^n l_0^{n+1/3} N_v$  we immediately obtain the corresponding update for  $\rho^{n+1/3}$  (using  $\mathbf{X}^\top \mathbf{X} = \mathbf{I}$ ):

$$\frac{\rho_0^{n+1/3} - \rho_0^n}{\Delta t} - \frac{1}{d} \sum_{k=1}^d \mathbf{X}^n \mathbf{A}_{\partial_k}^n (\mathbf{A}_\sigma^n)^{-1} \mathbf{A}_{\partial_k}^n (\mathbf{X}^n)^\top \rho_0^{n+1/3} = 0. \quad (39)$$

Perform the QR decomposition of  $\mathbf{L}^{n+1/3}$  to obtain the updated  $\mathbf{V}$  and  $\mathbf{S}$  at  $t + 1/3$ , and since  $\mathbf{V}$  will not change in later steps, we have:

$$\mathbf{V}^{n+1} = \mathbf{V}^{n+2/3} = \mathbf{V}^{n+1/3},$$

and according to (27):

$$\Gamma^{n+1} = \Gamma^{n+2/3} = \Gamma^{n+1/3} = (\mathbf{V}^\top \mathbf{C} \mathbf{V})^{n+1/3}, \quad \Xi^{n+1} = \Xi^{n+2/3} = \Xi^{n+1/3} = (\mathbf{V}^\top \Pi \mathbf{V})^{n+1/3}.$$

For convenience, we use the superscript  $(\cdot)^{n+1}$  uniformly for  $\mathbf{V}, \Gamma, \Xi$  in the following discussion. Without detailing the proof, see equations (63)-(67) in Appendix, we have:

- define  $\alpha^{n+1} = (\mathbf{V}^{n+1})^\top e$ , then

$$\text{null}\{\Gamma^{n+1}\} = \text{span}\{\alpha^{n+1}\}; \quad (40)$$

- there exists an orthogonal matrix  $\mathbf{Q} \in \mathbb{R}^{r \times r}$  such that

$$\alpha^{n+1,*} = \mathbf{Q}^\top \alpha^{n+1} = \left( \sqrt{N_v} + O(\epsilon^3), O(\epsilon^2), \dots, O(\epsilon^2) \right)^\top; \quad (41)$$

- use  $\mathbf{Q}$  from (41), further define  $\mathbf{V}^{n+1,*} = \mathbf{V} \mathbf{Q}$  and  $\Xi_{v_k}^{n+1,*} = \mathbf{Q}^\top \Xi_{v_k}^{n+1} \mathbf{Q}$ , then we have:

$$(\Xi_{v_k}^{n+1,*})_{1,j} = (\Xi_{v_k}^{n+1,*})_{j,1} = \frac{1}{\sqrt{d}} \delta_{k+1,j} + O(\epsilon), \quad 1 \leq j \leq d+1. \quad (42)$$

These assumptions naturally lead to

$$\alpha^\top \Xi_{v_m} \Xi_{v_n} \alpha = \frac{N_v}{d} \delta_{m,n} + O(\epsilon), \quad \text{and} \quad \alpha^\top \alpha = N_v. \quad (43)$$

**Step 2:** This step preserves  $\mathbf{X}$  and  $\mathbf{V}$  and updates  $\mathbf{L}$ . Thus, we plug the asymptotic expansion of  $\mathbf{S}$  into equation (25) and obtain

$$\begin{cases} O(1/\epsilon) : & \mathbf{A}_\sigma^n \mathbf{S}_0^{n+2/3} \Gamma^{n+1} = 0 \\ O(1) : & -\sum_{k=1}^d \mathbf{A}_{\partial_k}^n \mathbf{S}_0^{n+2/3} \Xi_{v_k}^{n+1} = -\mathbf{A}_\sigma^n \mathbf{S}_1^{n+2/3} \Gamma^{n+1}, \\ O(\epsilon) : & \frac{\mathbf{S}_0^{n+2/3} - \mathbf{S}_0^{n+1/3}}{\Delta t} - \sum_{k=1}^d \mathbf{A}_{\partial_k}^n \mathbf{S}_1^{n+2/3} \Xi_{v_k}^{n+1} = -\mathbf{A}_\sigma^0 \mathbf{S}_2^{n+2/3} \Gamma^{n+1} \end{cases}. \quad (44)$$

Since  $\mathbf{A}_\sigma^n$  is invertible, the leading order equation implies that  $\mathbf{S}_0^{n+2/3}$  lies in the null space of  $\Gamma^{n+1}$ . Thus, we have

$$\mathbf{S}_0^{n+2/3} = s_0^{n+2/3} (\alpha^{n+1})^\top, \quad (45)$$

where  $s_0^{n+2/3} \in \mathbb{R}^{r \times 1}$  is yet to be determined.

We now follow the same strategy as in step 1. That is, we plug the expression for  $\mathbf{S}_0^{n+2/3}$  into the equation of order  $\mathcal{O}(1)$  and then project out the null space of  $\Gamma^{n+1}$ .

$$\mathbf{S}_1^{n+2/3} = -\sum_{k=1}^d (\mathbf{A}_\sigma^n)^{-1} \mathbf{A}_{\partial_k}^n \mathbf{S}_0^{n+2/3} \Xi_{v_k}^{n+1} + s_1^{n+2/3} (\alpha^{n+1})^\top.$$

Then we close the system by plugging the result for  $\mathbf{S}_1^{n+2/3}$  into the equation of order  $\mathcal{O}(\epsilon)$ . This yields, using (43):

$$\frac{\mathbf{S}_0^{n+2/3} \alpha^{n+1} - \mathbf{S}_0^{n+1/3} \alpha^{n+1}}{\Delta t} + \frac{1}{d} \sum_{k=1}^d \mathbf{A}_{\partial_k}^n (\mathbf{A}_\sigma^n)^{-1} \mathbf{A}_{\partial_k}^n \mathbf{S}_0^{n+2/3} \alpha^{n+1} = 0. \quad (46)$$

Since we further have  $\mathbf{V}^{n+1} \alpha^{n+1} = e$ , by (63), we finally obtain

$$\frac{\rho_0^{n+2/3} - \rho_0^{n+1/3}}{\Delta t} + \frac{1}{d} \sum_{k=1}^d \mathbf{X}^n \mathbf{A}_{\partial_k}^n (\mathbf{A}_\sigma^n)^{-1} \mathbf{A}_{\partial_k}^n (\mathbf{X}^n)^\top \rho_0^{n+2/3} = 0, \quad (47)$$

where  $\rho_0^{n+2/3} = \mathbf{X}_0^n \mathbf{S}_0^{n+2/3} (\mathbf{V}_0^{n+2/3})^\top e$ . We then update the leading order of  $\mathbf{K}$  according to

$$\mathbf{K}_0^{n+2/3} = \mathbf{X}^n \mathbf{S}_0^{n+2/3} = \mathbf{X}^n s_0^{n+2/3} (\alpha^{n+1})^\top. \quad (48)$$

**Step 3:** This step preserves  $\mathbf{V}$  and updates  $\mathbf{K}$ . Thus, we plug the asymptotic expansion of  $\mathbf{K}$  into equation (29) and obtain

$$\begin{cases} O(1/\epsilon) : & \Sigma \mathbf{K}_0^{n+1} \Gamma^{n+1} = 0, \\ O(1) : & \sum_{k=1}^d \mathbf{D}_k \mathbf{K}_0^{n+1} \Xi_{v_k}^{n+1} = \Sigma \mathbf{K}_1^{n+1} \Gamma^{n+1} \\ O(\epsilon) : & \frac{\mathbf{K}_0^{n+1} - \mathbf{K}_0^{n+2/3}}{\Delta t} + \sum_{k=1}^d \mathbf{D}_k \mathbf{K}_1^{n+1} \Xi_{v_k}^{n+1} = \Sigma \mathbf{K}_2^{n+1} \Gamma^{n+1} \end{cases}. \quad (49)$$

Since  $\Sigma$  is invertible, the leading order equation implies that  $\mathbf{K}_0^{n+1}$  lies in the null space of  $\Gamma^{n+1}$ . Thus, we have

$$\mathbf{K}_0^{n+1} = k_0^{n+1} (\alpha^{n+1})^\top, \quad (50)$$

where  $k_0^{n+1} \in \mathbb{R}^{N_x \times 1}$  is yet to be determined. We now follow the same strategy as in step 1 and 2. That is, we plug the expression for  $\mathbf{K}_0^{n+1}$  into the equation of order  $\mathcal{O}(1)$  and then project out the null space of  $\Gamma^{n+1}$ . Then we close the system by plugging the result for  $\mathbf{K}_1^{n+2/3}$  into the equation of order  $\mathcal{O}(\epsilon)$ . This yields, once again

using (43):

$$\frac{\mathbf{K}_0^{n+1}\alpha^{n+1} - \mathbf{K}_0^{n+2/3}\alpha^{n+1}}{\Delta t} - \frac{1}{d} \sum_{k=1}^d \mathbf{D}_k \Sigma^{-1} \mathbf{D}_k \mathbf{K}_0^{n+1} \alpha^{n+1} = 0. \quad (51)$$

Now, since  $\rho_0^{n+1} = u_0^{n+1}e$  and  $u_0^{n+1} = \mathbf{K}_0^{n+1}(\mathbf{V}^{n+1})^\top = k_0^{n+1}\alpha^\top(\mathbf{V}^{n+1})^\top$ , we obtain, by using equation (43),

$$\frac{\rho_0^{n+1} - \rho_0^{n+2/3}}{\Delta t} - \frac{1}{d} \sum_{k=1}^d \mathbf{D}_k (\Sigma^{-1} \mathbf{D}_k \rho_0^{n+1}) = 0, \quad (52)$$

which concludes the proof for (34). To show (33), we denote  $\mathcal{L} = \sum_{k=1}^d \mathbf{X}^n \mathbf{A}_{\partial_k}^n (\mathbf{A}_\sigma^n)^{-1} \mathbf{A}_{\partial_k}^n (\mathbf{X}^n)^\top$ , then equation (39) and (47) can be written as

$$\rho_0^{n+2/3} = \left( \mathbf{I} + \frac{\Delta t}{d} \mathcal{L} \right)^{-1} \left( \mathbf{I} - \frac{\Delta t}{d} \mathcal{L} \right)^{-1} \rho_0^n = \left( \mathbf{I} - \frac{(\Delta t)^2}{d^2} \mathcal{L}^2 \right)^{-1} \rho_0^n. \quad (53)$$

By using  $(\mathbf{X}^n)^\top \mathbf{X}^n = \mathbf{I}$  we can bound  $\mathcal{L}$  as follows

$$\|\mathcal{L}\|_2 \leq C_d \frac{1}{(\Delta x)^2 \min(\sigma(x))},$$

with  $C_d$  being a constant depending on  $d$  only. Therefore,

$$\|\rho_0^{n+2/3} - \rho_0^n\|_2 = O\left(\frac{(\Delta t)^2}{(\Delta x)^2}\right) \Rightarrow \|\rho^{n+2/3} - \rho^n\|_2 = O\left(\frac{(\Delta t)^2}{(\Delta x)^2}\right) + O(\epsilon).$$

Finally, since

$$u_0^{n+1} = k_0^{n+1} \alpha^\top (\mathbf{V}^{n+1})^\top = k_0^{n+1} (e^\top \mathbf{V}^{n+1}) (\mathbf{V}_0^{n+1})^\top$$

we follow that  $e$  lies in the span of  $\mathbf{L}_0^{n+1/3}$  and thus in the span of  $\mathbf{V}_0^{n+1} = \mathbf{V}_0^{n+1/3}$ . We thus have  $u_0^{n+1} = k_0^{n+1} e^\top$ , as desired.  $\square$

**Remark 4.** We need certain assumptions for this statement to hold true. These assumptions are required to show that equations (40)-(42) are satisfied. However, since these assumptions are rather technical, we omit the details from the main text and refer the reader to the appendix for more details.

**3.3.2. Asymptotic analysis of the Crank–Nicolson scheme.** As observed in the previous section, the implicit Euler based low-rank algorithm can not be used as a time integrator. We will now show that the Crank–Nicolson approach is asymptotic preserving independent of the time step size  $\Delta t$  that is chosen.

**Theorem 3.** *Assuming that  $u^n = \rho_0^n e^\top + \mathcal{O}(\epsilon)$ , for some vector  $\rho_0^n \in \mathbb{R}^{r \times 1}$ . Employing the Crank–Nicolson method to compute  $u^{n+1}$  from  $u^n$ , using equation (23), (26) and (29), we asymptotically preserve the diffusion limit (3). More specifically, under some mild conditions (stated in Assumption 2 in Appendix), we have*

$$\|\rho^{n+2/3} - \rho^n\|_2 = O(\epsilon) \quad (54)$$

and

$$\frac{\rho_0^{n+1} - \rho_0^{n+2/3}}{\Delta t} - \frac{1}{d} \sum_{k=1}^d \mathbf{D}_k (\Sigma^{-1} \mathbf{D}_k \rho_0^{n+1}) = 0.$$

The latter is a discretization of the diffusion equation (3) using the implicit Euler method. Further, we have  $u^{n+1} = \rho_0^{n+1} e^\top$  for some vector  $\rho_0^{n+1} \in \mathbb{R}^{N_x \times 1}$ .

**Remark 5. The good.** It is immediate that Theorem 3 differs from Theorem 2 in that we preserve  $\rho$  in the limit  $\epsilon \rightarrow 0$  independent of the time step size. Note that both methods share the last step, which is responsible for propagating the diffusion equation.

**Remark 6. The bad.** The Crank–Nicolson based low-rank algorithm used here, although it “preserves” the asymptotic limit, is not able to drive the solution to the low-rank space. As stated in Theorem 3 we add the assumption that the initial value already has the corresponding structure of rank 1, up to an error of  $\mathcal{O}(\epsilon)$ , to ensure the initial data is well-prepared at each time step.

**Remark 7. The choice of  $D_k$**  We note that  $D_k(\Sigma^{-1}D_k)$  may not be self-adjoint operator in general if  $D_k$  is not chosen properly. In fact, if  $D_k$  is chosen as upwind type, the discretization is a shifted diffusion by one grid point in space. If  $D_k$  is chosen as central-scheme type, the self-adjoint property can be preserved, at the sacrifice of staggered behavior in the numerical solution. This type of problem is rather typical. A common way in the literature to overcome it by introducing the even-odd decomposition, the even part goes to the limit and the odd part diminishes. The two components are evolved with different type of fluxes [32]. Here numerically we simply balance the two types with a correctly chosen weight so that central scheme plays the major role in the diffusion limit. We leave the possible extension of introducing even-odd decomposition to future research.

*Proof.* Most of the proof is very similar to the case of the implicit Euler scheme detailed in Theorem 2. Thus, we will only highlight the main differences here and refer the reader to the appendix for a more thorough exposition.

The asymptotic expansion for the first step is given by

$$\begin{cases} \mathcal{O}(1/\epsilon) : & A_\sigma^n \left( L_0^{n+1/3} - L_0^n \right) C = 0 \\ \mathcal{O}(1) : & \sum_{k=1}^d A_{\partial_k}^n \left( L_0^{n+1/3} - L_0^n \right) \Pi_{v_k} = A_\sigma^n \left( L_1^{n+1/3} - L_1^n \right) C \\ \mathcal{O}(\epsilon) : & \frac{L_0^{n+1/3} - L_0^n}{\Delta t} + \sum_{k=1}^d A_{\partial_k}^n \left( L_1^{n+1/3} - L_1^n \right) \Pi_{v_k} = A_\sigma^n \left( L_2^{n+1/3} - L_2^n \right) C \end{cases} . \quad (55)$$

From the equation of order  $\mathcal{O}(1/\epsilon)$  we follow that

$$L_0^{n+1/3} = L_0^n + l_0^{n+1/3} e^\top .$$

Thus, we only know that the difference  $L_0^{n+1/3} - L_0^n$  lies in the null space of  $C^\top$ ; we can *not* make a similar claim for  $L_0^{n+1/3}$ . However, from the assumption  $u^n = \rho_0^n e^\top + \mathcal{O}(\epsilon)$  and from  $u^n = X^n L^n$  we immediately obtain  $L_0^n = l_0^n e^\top$ . This is an important ingredient in the remainder of the proof. It is also the first major difference between the present proof for the Crank–Nicolson method and the proof of Theorem 2, where this condition is automatically satisfied independent of the chosen initial value. Using similar arguments as in the proof of Theorem 2 we can then show (see Lemma 1 in the appendix for details):

- $L^n$  in (23) has the same form as (37).
- $S^{n+1/3}$  in (26) has the same form as (45).
- The equations for computing  $u_0^{n+1/3}$  and  $u_0^{n+2/3}$  (equations (80) and (81) in the appendix).

Further, see Appendix B for more details, we obtain

$$\begin{aligned}\rho_0^{n+1/3} &= \left(1 - \frac{(\Delta t)}{2d} \mathcal{L}^n\right)^{-1} \left(1 + \frac{(\Delta t)}{2d} \mathcal{L}^n\right) \rho_0^n, \\ \rho_0^{n+2/3} &= \left(1 + \frac{(\Delta t)}{2d} \mathcal{L}^n\right)^{-1} \left(1 - \frac{(\Delta t)}{2d} \mathcal{L}^n\right) \rho_0^{n+1/3},\end{aligned}$$

where as before  $\mathcal{L} = \sum_{k=1}^d \mathbf{X}^n \mathbf{A}_{\partial_k}^n (\mathbf{A}_{\sigma}^n)^{-1} \mathbf{A}_{\partial_k}^n (\mathbf{X}^n)^\top$ . Combining these two equations we get  $\rho_0^{n+2/3} = \rho_0^n$  for all  $n > 0$ , which is the desired result.  $\square$

As a summary, since the implicit Euler method is able to capture the low-rank structure of the diffusion limit, we use it in the first step of the algorithm. There we can choose the time step size, denoted by  $\Delta t_1$ , small enough such that the error term  $O((\Delta t_1)^2/(\Delta x)^2)$  is smaller than the desired accuracy. Since the method is only applied once, we do not have to worry about error propagation. All subsequent time steps, i.e. all steps from time  $t_1$  to time  $t_{\max}$  are then computed using the Crank–Nicolson approach. From Theorem 2 we know that after the first step all the prerequisites of Theorem 3 are satisfied and we thus conclude that the proposed numerical method is asymptotic preserving and is able to automatically capture the low-rank structure in the diffusion limit.

To show convergence we have to also show stability. However, for  $\epsilon \rightarrow 0$  our numerical method is simply given by the application of the implicit Euler method to a heat equation. Stability is thus a well known result as long as a proper space discretization is performed to obtain  $\mathbf{D}_k$ .

We summarize the final numerical method in Algorithm 1.

---

**Algorithm 1 (Dynamical low rank splitting method for the radiative transfer equation).**

---

**Preparation:**

1. Initial data:  $u(t=0, x, v)$ .
  2. Input data: final time:  $t_{\max}$ ; rank number:  $r$ ; time step:  $\Delta t_1 \leq \Delta t_2$ .
  3. Discretization points:  $\mathcal{X} = \{x_1, x_2, \dots, x_{N_x}\}, \mathcal{V} = \{v_1, v_2, \dots, v_{N_v}\}$
  4. Initialization: use SVD to construct initial  $u^0$  such that (11):  

$$u^0 = \mathbf{X}^0 \mathbf{S}^0 (\mathbf{V}^0)^T \approx u(t=0, x, v)$$
  5. Construct  $\Pi_{v_k}, \mathbf{C}$  by (24).
- Run:** set  $n = 0$ ;  
     call **Function implicit Euler** using  $\Delta t_1$  to update  $\mathbf{X}^1, \mathbf{S}^1, \mathbf{V}^1$ ;  
**While**  $t < t_{\max}$ :  $n \rightarrow n + 1$ ;  
     call **Function Crank–Nicolson** using  $\Delta t_2$  to obtain  $\mathbf{X}^{n+1}, \mathbf{S}^{n+1}, \mathbf{V}^{n+1}$ ;  
**end**  
**Output:** Numerical solution  $\mathbf{X}^n, \mathbf{S}^n$  and  $\mathbf{V}^n$  for  $t_n \leq t_{\max}$ .
- 

#### 4. NUMERICAL EXPERIMENTS

In this section we present some numerical evidence to demonstrate the behavior of the proposed dynamical low-rank integrator. Strictly speaking the radiative transfer equation is only defined for  $d \geq 2$ . However, in the quasi-2D case, assuming the data is homogeneous in  $y$ -direction, the equation degenerate to a problem with 1D

**Algorithm 2 (Function implicit Euler (22),(25),(29))****Input:**

1. time step  $\Delta t$ ;
2. Input data:  $\mathbf{X}^n$ ,  $\mathbf{S}^n$  and  $\mathbf{V}^n$ .

**Run:**

- Construct  $\mathbf{A}_{\partial_k}^n, \mathbf{A}_\sigma^n$  by (24); Compute  $\mathbf{L}^n = \mathbf{S}^n(\mathbf{V}^n)^\top$ ;
- Update  $\mathbf{L}^{n+1/3}$  by solving (22) with  $\Delta t_1$ ;
- Perform QR decomposition to obtain  $\mathbf{S}^{n+1/3}, \mathbf{V}^{n+1}$  from (22); Construct  $\Xi_{v_k}^{n+1}$  and  $\Gamma^{n+1}$  by (27);
- Update  $\mathbf{S}^{n+2/3}$  with  $\Delta t_1$  by solving (25);
- Construct  $\mathbf{K}^{n+2/3} = \mathbf{X}^n \mathbf{S}^{n+2/3}$  by (28);
- Update  $\mathbf{K}^{n+1}$  with  $\Delta t_1$  by solving (29);
- Perform QR decomposition to obtain  $\mathbf{X}^{n+1}, \mathbf{S}^{n+1}$  from (29);

**Output:** Numerical solution  $\mathbf{X}^{n+1}, \mathbf{S}^{n+1}, \mathbf{V}^{n+1}$ ;

**Algorithm 3 (Function Crank–Nicolson (23),(26),(29))****Input:**

1. time step  $\Delta t$ ;
2. Input data:  $\mathbf{X}^n$ ,  $\mathbf{S}^n$  and  $\mathbf{V}^n$ .

**Run:**

- Construct  $\mathbf{A}_{\partial_k}^n, \mathbf{A}_\sigma^n$  by (24); Compute  $\mathbf{L}^n = \mathbf{S}^n(\mathbf{V}^n)^\top$ ;
- Update  $\mathbf{L}^{n+1/3}$  by solving (23) with  $\Delta t$ ;
- Perform QR decomposition to obtain  $\mathbf{S}^{n+1/3}, \mathbf{V}^{n+1}$  from (23); Construct  $\Xi_{v_k}^{n+1}$  and  $\Gamma^{n+1}$  by (27);
- Update  $\mathbf{S}^{n+2/3}$  with  $\Delta t$  by solving (26);
- Construct  $\mathbf{K}^{n+2/3} = \mathbf{X}^n \mathbf{S}^{n+2/3}$  by (29);
- Update  $\mathbf{K}^{n+1}$  with  $\Delta t$  by solving (29);
- Perform QR decomposition to obtain  $\mathbf{X}^{n+1}, \mathbf{S}^{n+1}$  from (29); Set  $n = n + 1$  and  $t = t + \Delta t$ ;

**Output:** Numerical solution  $\mathbf{X}^{n+1}, \mathbf{S}^{n+1}, \mathbf{V}^{n+1}$ ;

in space as well. In this case the diffusion limit becomes:

$$\partial_t u = \frac{1}{3} \partial_x (\sigma^{-1}(x) \partial_x u), \quad (t, x) \in \mathbb{R}^+ \times \Omega_x. \quad (56)$$

To measure the error we define:

$$\mathcal{P}_{x,l}^{error} = \|u - \mathbf{X}_l(\mathbf{X}_l)^\top u\|_F \quad \text{and} \quad \mathcal{P}_{v,l}^{error} = \|u - u \mathbf{V}_l(\mathbf{V}_l)^\top\|_F, \quad (57)$$

where  $u$  is the reference solution and  $\mathbf{X}$  and  $\mathbf{V}$  are the numerical solution computed using the dynamic low rank integrator. The error is measured in the Frobenius norm for the matrix, which is equivalent to  $L_2(dx d\mu_v)$  in the continuous version.

**4.1. Projection error and singular value test.** Before testing the dynamic low rank numerical integrator, we first numerically justify that the solution is indeed of low rank. Setting the initial data to

$$f(0, x, v) = \begin{cases} 2, & 0.8 < x < 1.2 \\ 0, & \text{otherwise,} \end{cases}$$

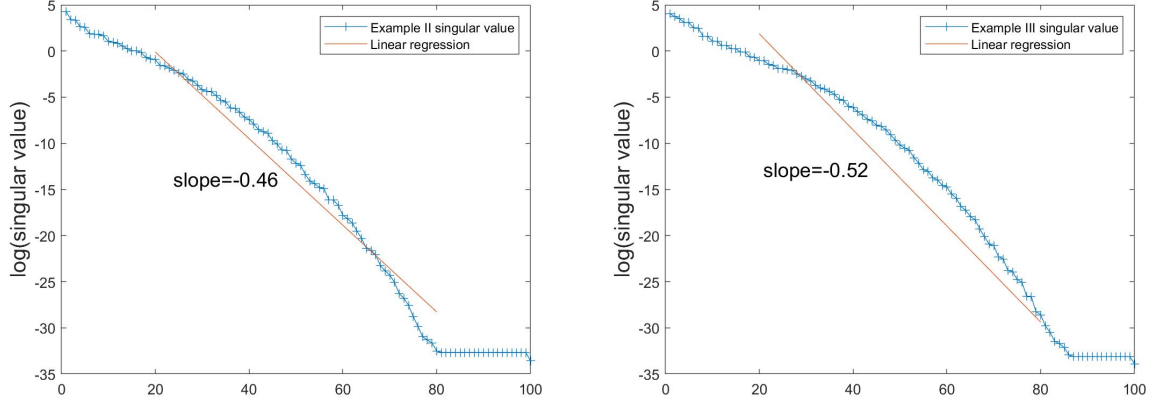


FIGURE 1. Here we use  $N_x = 200, N_v = 100$  and the direct implicit solver with upwind discretization for D to compute  $u$ . Left: Singular values of the solution  $u$  in Example II. Right: Singular values of the solution  $u$  in Example III.

with the equation equipped with isotropic scattering and a varying cross sections (see (61) and (62) below) at  $\epsilon = 1$ , we compute the equation with fine grids ( $N_x = 200$  and  $N_v = 100$ ) till  $t_{max} = 1$ . We plot the singular values of the solution in log-scale in Figure 1. It is clear that the singular values decay exponentially fast for both cases. This gives us the foundation to believe that the dynamical low rank approximation would work.

**4.2. Example I.** We consider a toy problem with the scattering cross section a constant

$$\sigma(x) = 2, \quad x \in [0, 2].$$

and the initial condition set as:

$$f(0, x, v) = ((x - 1)^2 + 1) (v^2 + 1). \quad (58)$$

In running Algorithm 1, the dynamical low rank approximation, we combines central difference and upwind (CCP) flux for D, namely:

$$(Du^n)_{i,j} = \begin{cases} \epsilon \frac{u_i^n - u_{i-1}^n}{\Delta x} + (1 - \epsilon) \frac{u_{i+1}^n - u_{i-1}^n}{2\Delta x}, & v_j > 0 \\ \epsilon \frac{u_{i+1}^n - u_i^n}{\Delta x} + (1 - \epsilon) \frac{u_{i+1}^n - u_{i-1}^n}{2\Delta x}, & v_j \leq 0 \end{cases}. \quad (59)$$

The combination factor is determined by the Knudsen number  $\epsilon$ . This means in the kinetic regime when  $\epsilon$  is close to 1 the flux becomes purely upwind but in the diffusion regime when  $\epsilon \rightarrow 0$ , the scheme is of central type. In the kinetic regime for  $\epsilon = 1$ , we set  $N_x = 200$  and  $N_v = 100$  for computing the reference solution, and we compare the low rank integrator solution with  $r = 20$  and the same  $(N_x, N_v)$  to this reference solution. In the diffusion regime, for  $\epsilon = 10^{-3}$ , the reference solution is given by the numerical solution to the diffusion equation directly. Both cases are shown in Figure 2 (for  $t_{max} = 1$  and  $t_{max} = 0.1$  respectively) where we clearly see the good fit.

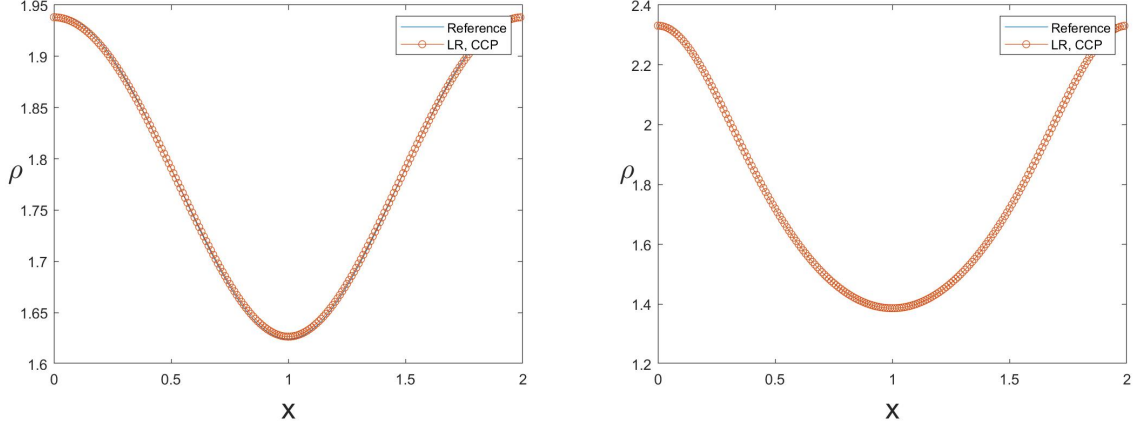


FIGURE 2. Example I. We set  $N_x = 200, N_v = 100, r = 20$ . Left:  $\epsilon = 1$ , we compare the density  $\rho$  from the dynamical low-rank algorithm with a reference solution at  $t_{\max} = 1$ . Right:  $\epsilon = 10^{-3}$ , we compare the density  $\rho$  from the dynamical low rank algorithm with diffusion limit at  $t_{\max} = 0.1$ .

We realize the upwind flux typically brings high artificial diffusion, and this diffusion would be magnified in the diffusion equation when the flux term becomes stiff. To justify the choice of flux  $D$  defined above, here we compute the solution using dynamic low rank approximation with  $D$  simply set as the upwind type. The results are shown in Figure 3. For relatively big Knudsen number ( $\epsilon = 1$ ), the low rank integrator solution still agrees with the reference solution well, but the behavior significantly deteriorates in the diffusion regime when  $\epsilon \rightarrow 0$ . This is expected as stated in Remark 7 that the stencil for the upwind scheme is not symmetric, leading to the fact that  $D(\Sigma^{-1}D)$  is not a self-adjoint operator as it should be for the  $\epsilon \rightarrow 0$  limit.

4.3. **Example II.** We consider the following initial condition:

$$f(0, x, v) = \begin{cases} 2, & 0.8 < x < 1.2 \\ 0, & \text{otherwise,} \end{cases} \quad (60)$$

and isotropic scattering with a cross section

$$\sigma(x) = 100(x - 1)^4. \quad (61)$$

The cross section thus become critical at  $x = 1$ . Comparing the dynamical low rank solution using  $r = 20$  to the reference solution (fine discretization for  $\epsilon = 1$  and diffusion limit for  $\epsilon = 10^{-3}$ ), we see good agreement, as shown in Figure 4. To be quantitative, we also plot the error, defined in (57), in Figure 5. It is clear that the error decays exponentially fast. We also test the dynamic low rank integrator with  $D$  set to be of central scheme type. In this case, however, the method provides lots of artificial oscillation, as shown in Figure 6. These artificial oscillations do seem to capture the reference solution weakly (with oscillations centered around the true solution).

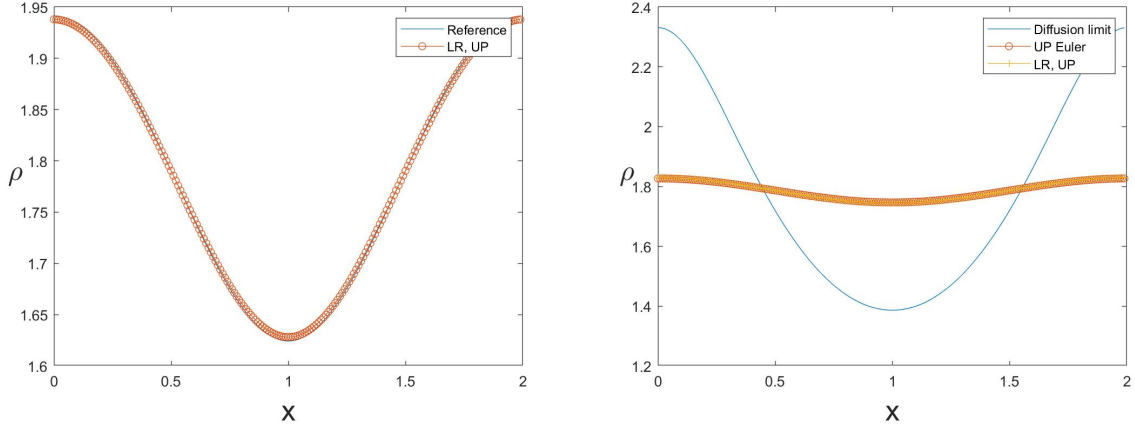


FIGURE 3. Example I. Here  $N_x = 200, N_v = 100, r = 20$ . Left:  $\epsilon = 1$ , we compare the reference solution and the dynamic low rank integrator solution with upwinding type of flux at  $t_{\max} = 1$ . Right:  $\epsilon = 10^{-3}$ , we compare the solution to the diffusion equation with the dynamic low rank integrator solution with upwinding type of flux at  $t_{\max} = 0.1$ .

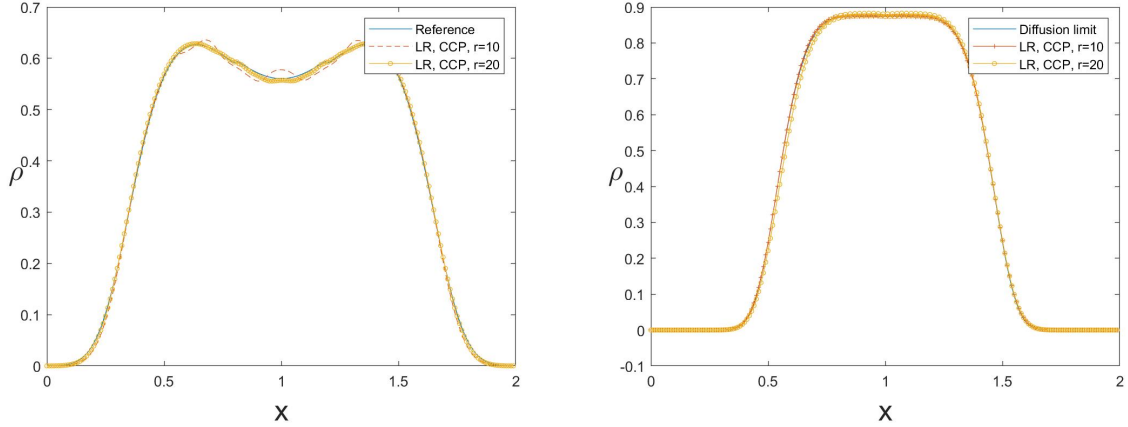


FIGURE 4. Example II. Here  $N_x = 200, N_v = 100$ . Left:  $\epsilon = 1$  and  $r = 10, 20$ , we compare the density  $\rho$  from the low-rank algorithm using CCP for  $D_k$  with the implicit Euler/upwind solver at  $t_{\max} = 1$ . Right:  $\epsilon = 10^{-3}$  and  $r = 10, 20$ , we compare the density  $\rho$  from the low-rank algorithm using CCP with the diffusion limit at  $t_{\max} = 0.1$ . In the plots, LR stands for dynamic low rank solution.

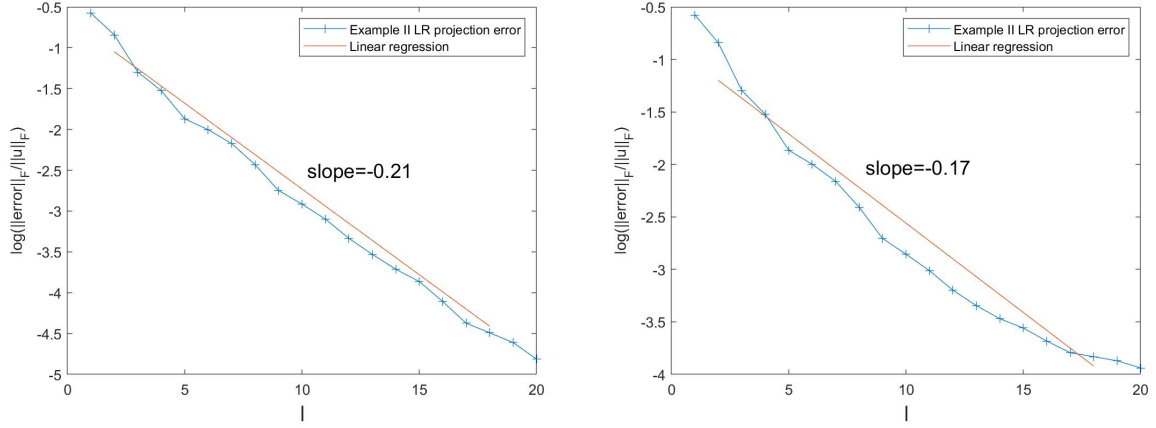


FIGURE 5. Example II. Here we use  $N_x = 200, N_v = 100, r = 20$ . The numerical solution  $u$  is computed using the implicit Euler/upwind solver and  $\mathbf{X}, \mathbf{V}$  is computed using the low-rank algorithm. Left:  $\log\left(\frac{\mathcal{P}_{x,l}^{error}}{\|u\|_F}\right)$  as a function of  $l$ . Right:  $\log\left(\frac{\mathcal{P}_{v,l}^{error}}{\|u\|_F}\right)$  as a function of  $l$ .

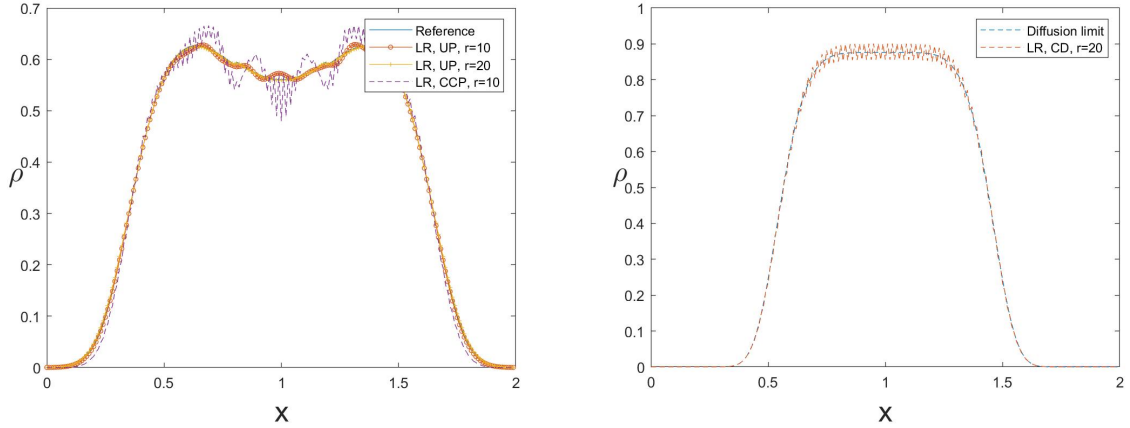


FIGURE 6. Example II. Here  $N_x = 200, N_v = 100$ . Left:  $\epsilon = 1$  and  $r = 10, 20$ , we compare the density  $\rho$  from the low-rank algorithm using upwind and central differences for  $D_k$  with the implicit Euler/upwind solver at  $t_{\max} = 1$ . Right:  $\epsilon = 10^{-3}$  and  $r = 20$ , we compare the density  $\rho$  from the low-rank algorithm using central differences with the diffusion limit at  $t_{\max} = 0.1$ . In the plots, LR stands for dynamic low rank solution, and CS stands for central scheme, while UP stands for upwinding.

4.4. **Example III.** In the third example, we use the same initial condition as in Example II, but modify the cross section:

$$\sigma(x) = \begin{cases} 0.02, & x \in [0.35, 0.65] \cup [1.35, 1.65] \\ 1, & x \in [0, 0.35) \cup (0.65, 1.35) \cup (1.65, 2] \end{cases}. \quad (62)$$

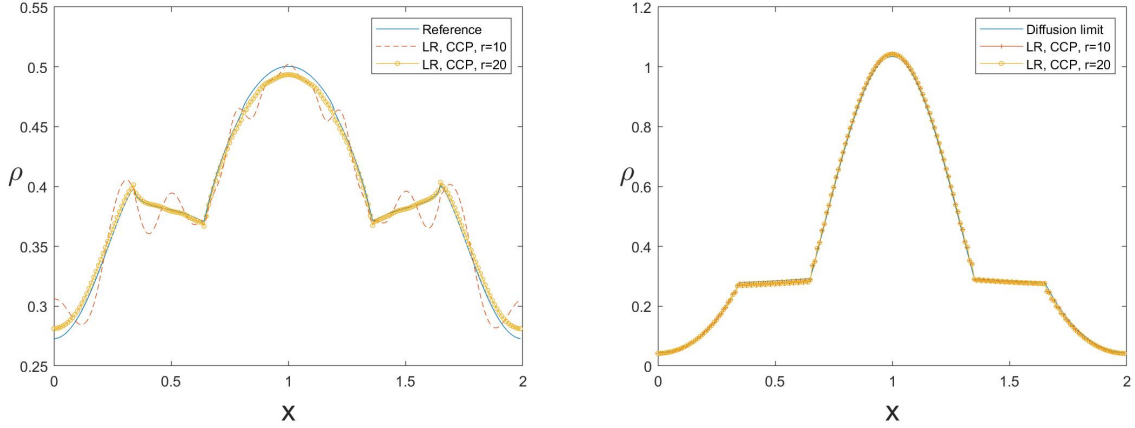


FIGURE 7. Example III. Here  $N_x = 200, N_v = 100$ . Left:  $\epsilon = 1$  and  $r = 10, 20$ , we compare the density  $\rho$  from the low-rank algorithm using CCP for  $D_k$  with the implicit Euler/upwind solver at  $t_{\max} = 1$ . Right:  $\epsilon = 10^{-3}$  and  $r = 10, 20$ , we compare the density  $\rho$  from the low-rank algorithm using CCP with the diffusion limit at  $t_{\max} = 0.1$ .

This cross section is of high contrast and has a discontinuity, and thus the equation quickly achieves equilibrium in the optical thick region ( $\sigma \sim 1$ ), while still staying in the kinetic regime in the optical thin region ( $\sigma \sim 0.02$ ). The dynamic low rank integrator uses  $r = 20$ . To obtain the reference solutions, we either compute the equation with fine grid when  $\epsilon = 1$ , or compute the diffusion equation directly with  $\epsilon = 10^{-3}$ . We also compute the error: it decays exponentially fast, as plotted in Figure 8.

**Acknowledgement.** The work of ZD and QL is supported in part by Wisconsin Data Science Initiative, and National Science Foundation under the grant DMS-1619778, 1750488, RNMS KI-NET 1107291, and TRIPODS: 1740707.

#### REFERENCES

- [1] A. Arnold and T. Jahnke. On the approximation of high-dimensional differential equations in the hierarchical Tucker format. *BIT Numer. Math.*, 54(2):305–341, 2014.
- [2] C. Bardos, R. Santos, and R. Sentis. Diffusion approximation and computation of the critical size. *Trans. Amer. Math. Soc.*, 284(2):617–649, 1984.
- [3] M. Bennoune, M. Lemou, and L. Mieussens. Uniformly stable numerical schemes for the Boltzmann equation preserving the compressible Navier-Stokes asymptotics. *J. Comput. Phys.*, 227:3781–3803, 2008.
- [4] D. Conte and C. Lubich. An error analysis of the multi-configuration time-dependent Hartree method of quantum dynamics. *ESAIM Math. Model. Numer. Anal.*, 44(4):759–780, 2010.
- [5] N. Crouseilles, M. Mehrenberger, and F. Vecil. Discontinuous Galerkin semi-Lagrangian method for Vlasov-Poisson. In *ESAIM: Proceedings*, volume 32, pages 211–230, 2011.
- [6] W. Dahmen, R. DeVore, L. Grasedyck, and E. Süli. Tensor-sparsity of solutions to high-dimensional elliptic partial differential equations. *Found. Comput. Math.*, 16(4):813–874, 2016.

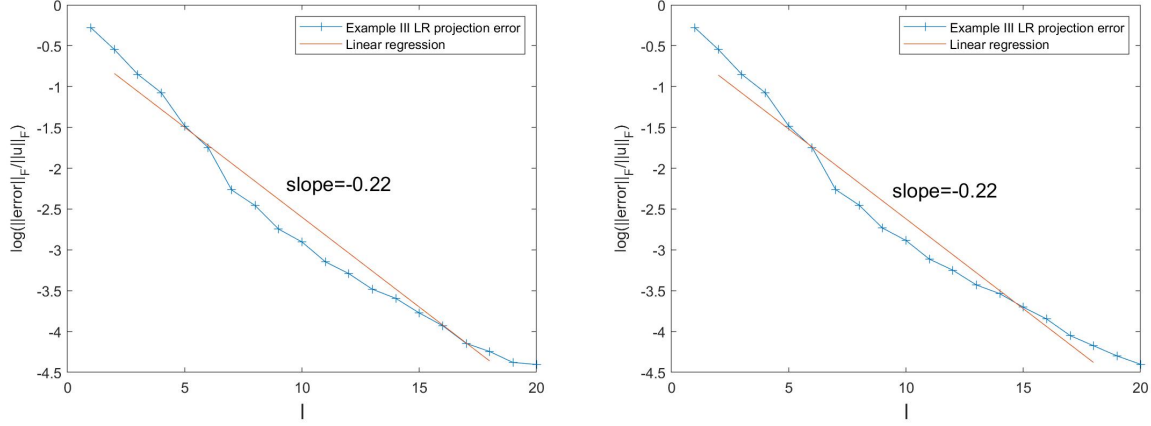


FIGURE 8. Example III. Here we use  $N_x = 200, N_v = 100, r = 20$ . the numerical solution  $u$  is computed using the implicit Euler/upwind solver and  $\mathbf{X}, \mathbf{V}$  is computed using the low-rank algorithm. Left:  $\log\left(\frac{\mathcal{P}_{x,l}^{error}}{\|u\|_F}\right)$  as a function of  $l$ . Right:  $\log\left(\frac{\mathcal{P}_{v,l}^{error}}{\|u\|_F}\right)$  as a function of  $l$ .

- [7] P. Degond, S. Jin, and J.G. Liu. Mach-number uniform asymptotic-preserving gauge schemes for compressible flows. *Bull. Inst. Math. Acad. Sin. (N.S.)*, 2, 01 2007.
- [8] Pierre Degond, Fabrice Deluzet, Laurent Navoret, An-Bang Sun, and Marie-Helene Vignal. Asymptotic-preserving particle-in-cell method for the vlasovpoisson system near quasineutrality. *Journal of Computational Physics*, 229(16):5630 – 5652, 2010.
- [9] G. Dimarco and L. Pareschi. Exponential Runge-Kutta methods for stiff kinetic equations. *SIAM Journal on Numerical Analysis*, 49(1):2057–2077, 2011.
- [10] G. Dimarco and L. Pareschi. Numerical methods for kinetic equations. *Acta Numer.*, 23:369–520, 2014.
- [11] L. Einkemmer. A low-rank algorithm for weakly compressible flow. arXiv:1804.04561.
- [12] L. Einkemmer. High performance computing aspects of a dimension independent semi-Lagrangian discontinuous Galerkin code. *Comput. Phys. Commun.*, 202:326–336, 2016.
- [13] L. Einkemmer. A performance comparison of semi-Lagrangian discontinuous Galerkin and spline based Vlasov solvers in four dimensions. *J. Comput. Phys.*, 376:937–951, 2019.
- [14] L. Einkemmer and C. Lubich. A quasi-conservative dynamical low-rank algorithm for the Vlasov equation. arXiv:1807.02338.
- [15] L. Einkemmer and C. Lubich. A low-rank projector-splitting integrator for the Vlasov–Poisson equation. *SIAM J. Sci. Comput.*, 40:B1330–B1360, 2018.
- [16] L. Einkemmer, A. Ostermann, and C. Piazzola. A low-rank projector-splitting integrator for the Vlasov–Maxwell equations with divergence correction. arXiv:1902.00424, 2019.
- [17] F. Filbet and E. Sonnendrücker. Comparison of Eulerian Vlasov solvers. *Comput. Phys. Commun.*, 150(3):247–266, 2003.
- [18] V. Grandgirard, J. Abiteboul, J. Bigot, T. Cartier-Michaud, N. Crouseilles, G. Dif-Pradalier, Ch. Ehrlacher, D. Esteve, X. Garbet, Ph. Ghendrih, G. Latu, M. Mehrenberger, C. Norscini, C. Passeron, F. Rozar, Y. Sarazin, E. Sonnendrücker, A. Strugarek, and D. Zaroso. A 5D gyrokinetic full-f global semi-Lagrangian code for flux-driven ion turbulence simulations. *Comput. Phys. Commun.*, 207:35–68, 2016.
- [19] J. Haegeman, C. Lubich, I. Oseledets, B. Vandereycken, and F. Verstraete. Unifying time evolution and optimization with matrix product states. *Physical Review B*, 94(16):165116, 2016.

- [20] J. Hu, S. Jin, and Q. Li. Chapter 5 - Asymptotic-Preserving Schemes for Multiscale Hyperbolic and Kinetic Equations. In R. Abgrall and C. Shu, editors, *Handbook of Numerical Methods for Hyperbolic Problems*, volume 18 of *Handbook of Numerical Analysis*, pages 103 – 129. Elsevier, 2017.
- [21] S. Jin. Efficient Asymptotic-Preserving (AP) Schemes For Some Multiscale Kinetic Equations. *SIAM J. Sci. Comput.*, 21(2):441–454, 1999.
- [22] S. Jin and C.D. Levermore. Numerical Schemes for Hyperbolic Conservation Laws with Stiff Relaxation Terms. *J. Comput. Phys.*, 126(2):449 – 467, 1996.
- [23] S. Jin and L. Pareschi. Asymptotic-Preserving (AP) Schemes for Multiscale Kinetic Equations: a Unified Approach. In H. Freistühler and G. Warnecke, editors, *Hyperbolic Problems: Theory, Numerics, Applications*, pages 573–582. Birkhäuser Basel, Basel, 2001.
- [24] S. Jin, L. Pareschi, and G. Toscani. Uniformly accurate diffusive relaxation schemes for multiscale transport equations. *SIAM J. Numer. Anal.*, 38(3):913–936, 2000.
- [25] E. Kieri, C. Lubich, and H. Walach. Discretized dynamical low-rank approximation in the presence of small singular values. *SIAM J. Numer. Anal.*, 54(2):1020–1038, 2016.
- [26] O. Koch and C. Lubich. Dynamical low-rank approximation. *SIAM J. Matrix Anal. Appl.*, 29(2):434–454, 2007.
- [27] O. Koch and C. Lubich. Dynamical tensor approximation. *SIAM J. Matrix Anal. Appl.*, 31(5):2360–2375, 2010.
- [28] K. Kormann. A semi-Lagrangian Vlasov solver in tensor train format. *SIAM J. Sci. Comput.*, 37(4):613–632, 2015.
- [29] E.W. Larsen, J.E. Morel, and W.F. Miller. Asymptotic solutions of numerical transport problems in optically thick, diffusive regimes. *J. Comput. Phys.*, 69(2):283 – 324, 1987.
- [30] M. Lemou and L. Mieussens. A new asymptotic preserving scheme based on micro-macro formulation for linear kinetic equations in the diffusion limit. *SIAM J. Sci. Comput.*, 31:334–368, 2008.
- [31] Q. Li and L. Pareschi. Exponential Runge-Kutta for the inhomogeneous Boltzmann equations with high order of accuracy. *J. Comput. Phys.*, 259:402–420, 2014.
- [32] Q. Li and L. Wang. Implicit Asymptotic Preserving Method for Linear Transport Equations. *Commun. Comput. Phys.*, 22(1):157–181, 2017.
- [33] C. Lubich. *From quantum to classical molecular dynamics: reduced models and numerical analysis*. European Mathematical Society, 2008.
- [34] C. Lubich. Time integration in the multiconfiguration time-dependent Hartree method of molecular quantum dynamics. *Applied Mathematics Research eXpress*, 2015(2):311–328, 2015.
- [35] C. Lubich, I. V. Oseledets, and B. Vandereycken. Time integration of tensor trains. *SIAM J. Numer. Anal.*, 53(2):917–941, 2015.
- [36] C. Lubich and I.V. Oseledets. A projector-splitting integrator for dynamical low-rank approximation. *BIT Numer. Math.*, 54(1):171–188, 2014.
- [37] C. Lubich, T. Rohwedder, R. Schneider, and B. Vandereycken. Dynamical approximation by hierarchical Tucker and tensor-train tensors. *SIAM J. Matrix Anal. Appl.*, 34(2):470–494, 2013.
- [38] C. Lubich, B. Vandereycken, and H. Walach. Time integration of rank-constrained tucker tensors. *SIAM J. Numer. Anal.*, 56(3):1273–1290, 2018.
- [39] H.-D. Meyer, F. Gatti, and G. A. Worth. *Multidimensional quantum dynamics*. John Wiley & Sons, 2009.
- [40] H.-D. Meyer, U. Manthe, and L. S. Cederbaum. The multi-configurational time-dependent Hartree approach. *Chem. Phys. Letters*, 165(1):73–78, 1990.
- [41] C. Mouhot and C. Villani. On landau damping. *Acta Math.*, 207(1):29–201, Sep 2011.
- [42] A. Nonnenmacher and C. Lubich. Dynamical low-rank approximation: applications and numerical experiments. *Math. Comput. Simul.*, 79(4):1346 – 1357, 2008.
- [43] A. Ostermann, C. Piazzola, and H. Walach. Convergence of a low-rank lie–trotter splitting for stiff matrix differential equations. *arXiv:1803.10473*, 2018.
- [44] N. J. Sircombe and T. D. Arber. VALIS: A split-conservative scheme for the relativistic 2D Vlasov–Maxwell system. *J. Comput. Phys.*, 228(13):4773–4788, 2009.

- [45] D. Ter Haar. *Men of physics: L.D. Landau*, volume 2. Elsevier, 1969.

## APPENDIX A. ASSUMPTIONS IN THEOREM 2

The technical assumptions used in Theorem 2 are as follows.

**Assumption 1.** *There exists an orthogonal matrix  $Q \in \mathbb{R}^{r \times r}$  such that*

$$\mathbf{V}^{n+1,*} = \mathbf{V}^{n+1}Q = \left( e/\sqrt{N_v} + \epsilon^2 a_0 + O(\epsilon^3), \frac{\sqrt{d}}{\sqrt{N_v}} \mathcal{V}_1 + \epsilon a_1 + O(\epsilon^2), \frac{\sqrt{d}}{\sqrt{N_v}} \mathcal{V}_2 + \epsilon a_2 + O(\epsilon^2), \dots, \right. \\ \left. \frac{\sqrt{d}}{\sqrt{N_v}} \mathcal{V}_d + \epsilon a_d + O(\epsilon^2), V_{d+2}^*, \dots, V_r^* \right) \quad (63)$$

with  $a_0, a_1, \dots, a_d \in \mathbb{R}^{N_v}$  satisfying

$$e^T a_k = O(\epsilon), (\mathcal{V}_k)^T V_i^{n+1,*} = O(\epsilon), e^T V_i^{n+1,*} = O(\epsilon^2), 1 \leq k \leq d, i \geq d+2, \quad (64)$$

$$e^T a_0 = O(\epsilon), \alpha^{n+1,*} = (\mathbf{V}^{n+1,*})^T e = \left( \sqrt{N_v} + O(\epsilon^3), O(\epsilon^2), \dots, O(\epsilon^2) \right)^T. \quad (65)$$

Note that conditions (64),(65) guarantee the orthonormality of  $V^{1,*}$ . Now, using equation (65) and denoting  $\alpha^{n+1,*} = Q^T \alpha^{n+1}$  we have

$$\alpha^{n+1,*}(\alpha^{n+1,*})^T = Q^T \alpha^{n+1}(\alpha^{n+1})^T Q, (\alpha^{n+1,*})^T \alpha^{n+1,*} = (\alpha^{n+1})^T \alpha^{n+1} = N_v + O(\epsilon^3). \quad (66)$$

For each  $1 \leq k \leq d$  we define

$$\Xi_{v_k}^{n+1,*} = (\mathbf{V}^{n+1,*})^T \text{diag}(\mathcal{V}_k) \mathbf{V}^{n+1,*}$$

Then we get

$$\Xi_{v_k}^{n+1,*} = Q^T \Xi_{v_k}^{n+1} Q, (\Xi_{v_k}^{n+1,*})_{1,j} = (\Xi_{v_k}^{n+1,*})_{j,1} = \frac{1}{\sqrt{d}} \delta_{k+1,j} + O(\epsilon), 1 \leq j \leq d+1, \quad (67)$$

where the second equality can be shown by using equation (65).

## APPENDIX B. DETAILS FOR THE PROOF OF THEOREM 3

Similar to Assumption 1, we first need to make the following assumption (for  $n > 0$ ).

**Assumption 2.** *For any  $n > 0$ , there exists an orthogonal matrix  $Q^{n+1} \in \mathbb{R}^{r \times r}$  such that*

$$\mathbf{V}^{n+1,*} = \mathbf{V}^{n+1}Q^{n+1} = \left( e/\sqrt{N_v} + \epsilon^2 a_0 + O(\epsilon^4), \frac{\sqrt{d}}{\sqrt{N_v}} \mathcal{V}_1 + \epsilon a_1^{n+1} + O(\epsilon^2), \frac{\sqrt{d}}{\sqrt{N_v}} \mathcal{V}_2 + \epsilon a_2^{n+1} + O(\epsilon^2), \dots, \right. \\ \left. \frac{\sqrt{d}}{\sqrt{N_v}} \mathcal{V}_d + \epsilon a_d^{n+1} + O(\epsilon^2), V_{d+2}^{n+1,*}, \dots, V_r^{n+1,*} \right) \quad (68)$$

with  $a_0, a_1, \dots, a_d \in \mathbb{R}^{N_v}$  satisfying

$$e^T a_j^{n+1} = O(\epsilon), (\mathcal{V}_k)^T V_i^{n+1,*} = O(\epsilon), e^T V_i^{n+1,*} = O(\epsilon^2), 0 \leq j \leq d, 1 \leq k \leq d, i \geq d+2, \quad (69)$$

$$\alpha^{n+1,*} = (\mathbf{V}^{n+1,*})^T e = \left( \sqrt{N_v} + O(\epsilon^3), O(\epsilon^2), \dots, O(\epsilon^2) \right)^T. \quad (70)$$

**Lemma 1.** *If Assumption 2 holds true, then for all  $n > 0$ ,  $\mathbf{L}_0^n$  and  $\mathbf{S}_0^{n+1/3}$  can be written as follows*

$$\mathbf{L}_0^n = l_0^n e^T, \quad \mathbf{S}_0^{n+1/3} = s_0^{n+1/3} (\alpha^{n+1})^T, \quad \alpha^{n+1} = \mathbf{V}^{n+1} e^T, \quad (71)$$

with some  $l_0^n \in \mathbb{R}^{r \times 1}$  and  $s_0^{n+1/3} \in \mathbb{R}^{r \times 1}$ .

**Remark 8.** Using Assumption 2 and Lemma 1, we can further prove that in each step,  $\mathbf{L}^{n+1/3}$  can be written as

$$\mathbf{L}^{n+1/3} = \hat{l}^{n+1/3} e^T - \epsilon \sum_{k=1}^d (A_\sigma^n)^{-1} A_{\partial_k}^n \hat{l}^{n+1/3} e^T \Pi_{v_k} + O(\epsilon^2), \quad (72)$$

where  $\hat{l}^{n+1/3} = l_0^{n+1/3} + \epsilon l_1^{n+1/3}$ .

*Proof.* The proof proceeds by induction. First, for  $n = 1$ , by (50), after doing QR decomposition, we obtain

$$\mathbf{S}_0^1 = s e_{1,r} (\alpha^1)^T, \quad e_{1,r} = (1, 0, \dots, 0)^T \in \mathbb{R}^{r \times 1}, \quad (73)$$

where  $s$  is a number and  $\alpha^1 = (\mathbf{V}^1)^T e$ . Using Assumption 2 we then get

$$\mathbf{L}_0^1 = s^1 e_{1,r} (\alpha^1)^T (\mathbf{V}^1)^T + O(\epsilon) = s^1 e_{1,r} (\alpha^{1,*})^T (\mathbf{V}^{1,*})^T + O(\epsilon) = s^1 e_{1,r} e^T + O(\epsilon) \quad (74)$$

If we consider terms of order  $O(1/\epsilon)$  in the asymptotic expansion of equation (23), we obtain

$$\mathbf{L}_0^{4/3} + \mathbf{L}_0^1 = l_0^{4/3} e^T + l_0^1 e^T. \quad (75)$$

After performing the QR decomposition we have

$$\mathbf{S}_0^{4/3} = \mathbf{L}_0^{n+1/3} \mathbf{V}^2 + O(\epsilon) = l_0^{4/3} e^T \mathbf{V}^2 + O(\epsilon) = l_0^{4/3} (\alpha^2)^T + O(\epsilon). \quad (76)$$

This shows that equation (71) holds true for  $n = 1$ .

Now if for  $n = k - 1$  equation (71) holds true, then we can show that

$$\mathbf{L}_0^k = l_0^k e^T, \quad (77)$$

which implies

$$\mathbf{L}_0^{k+1/3} + \mathbf{L}_0^k = l_0^{k+1/3} e^T + l_0^k e^T. \quad (78)$$

Then we perform a QR decomposition and obtain

$$\mathbf{S}_0^{k+1/3} = s_0^{k+1/3} (\alpha^{n+1})^T, \quad (79)$$

where  $s_0^{k+1/3} = l_0^{k+1/3}$ . □

We now, consider the proof of Theorem 3 in more detail.

*Proof. Step 1-2:* Instead of (39) and (47). We can obtain

$$\frac{u_0^{n+1/3} e - u_0^n e}{\Delta t} - \frac{1}{d} \sum_{k=1}^d \mathbf{X}^n \mathbf{A}_{\partial_k}^n (\mathbf{A}_\sigma^n)^{-1} \mathbf{A}_{\partial_k}^n (\mathbf{X}^n)^T \frac{u_0^{n+1/3} e + u_0^n e}{2} = 0, \quad (80)$$

$$\frac{u_0^{n+2/3} e - u_0^{n+1/3} e}{\Delta t} + \frac{1}{d} \sum_{k=1}^d \mathbf{X}^n \mathbf{A}_{\partial_k}^n (\mathbf{A}_\sigma^n)^{-1} \mathbf{A}_{\partial_k}^n (\mathbf{X}^n)^T \frac{u_0^{n+2/3} e + u_0^{n+1/3} e}{2} = 0 \quad (81)$$

This gives us

$$\rho_0^{n+1/3} = \left( I - \frac{(\Delta t)}{2d} \mathcal{L}^n \right)^{-1} \left( I + \frac{(\Delta t)}{2d} \mathcal{L}^n \right) \rho_0^n, \quad (82)$$

$$\rho_0^{n+2/3} = \left( I + \frac{(\Delta t)}{2d} \mathcal{L}^n \right)^{-1} \left( I - \frac{(\Delta t)}{2d} \mathcal{L}^n \right) \rho_0^{n+1/3} \quad (83)$$

$$\Rightarrow \rho_0^{n+2/3} = \rho_0^n. \quad (84)$$

Now, instead of (33), we obtain

$$\rho_0^{n+2/3} = \rho_0^n, \quad \text{for } n > 0. \quad (85)$$

in the first two splitting step with Crank–Nicolson scheme.

**Step 3:** Using equation (71) we have

$$S_0^{n+1/3} = s_0^{n+1/3} (\alpha^{n+1})^T. \quad (86)$$

From the terms of order  $O(1/\epsilon)$  we then obtain

$$S_0^{n+2/3} = s_0^{n+2/3} (\alpha^{n+1})^T \Rightarrow K_0^{n+2/3} = k_0^{n+2/3} (\alpha^{n+1})^T. \quad (87)$$

Repeating the procedure used to derive equations (51)–(52), we still recover the diffusion limit in the last splitting step as

$$\frac{\rho_0^{n+1} - \rho_0^{n+2/3}}{\Delta t} - \sum_{k=1}^d D_k \left( \frac{1}{d \cdot \text{diag}(\sigma(\mathcal{X}))} D_k \rho_0^{n+1} \right) = 0. \quad (88)$$

□

### APPENDIX C. DISCUSSION ABOUT ASSUMPTION

In this section, we will focus on Assumptions 1 and 2. First, by considering equations (38) and (72), it suffices to show that the space spanned by the rows of  $\hat{l}^{n+1/3} e^T - \epsilon \sum_{k=1}^d (A_\sigma^n)^{-1} A_{\partial_k}^n \hat{l}^{n+1/3} e^T \Pi_{v_k}$  can contain  $e^T, \mathcal{V}_1^T, \dots, \mathcal{V}_d^T$ . This, in turn, is equivalent to show that the following  $\mathbb{R}^{r \times (d+1)}$  matrix has at least rank  $d+1$

$$\Gamma = \left( A_\sigma^n \hat{l}^{n+1/3}, A_{\partial_1}^n \hat{l}^{n+1/3}, \dots, A_{\partial_d}^n \hat{l}^{n+1/3} \right). \quad (89)$$

For convenience, we only consider  $\sigma(x) = 1$  and  $D_k$  is discretized by centered differences. First, we define the operator  $\mathcal{H} : \mathbb{R}^{N_x \times 1} \rightarrow \mathbb{R}^{d \times d}$  as follows

$$(\mathcal{H}(U))_{i,j} = (D_i U)^T (D_j U), \quad U \in \mathbb{R}^{N_x \times 1} \quad (90)$$

which can be considered as the discretization of

$$\int_{\Omega_x} \nabla u (\nabla u)^T dx, \quad (91)$$

where  $u : \mathbb{R}^d \rightarrow \mathbb{R}$ . In this framework we can show the following lemma.

**Lemma 2.** *If Assumption 2 is true for the numerical solution at time  $t_n$  and we have*

$$\det(\mathcal{H}(k^n)) \neq 0, \quad (92)$$

where  $k^n$  is defined in equation (50). Then with small enough  $\frac{\Delta t}{(\Delta x)^2}$  and  $\epsilon$ , Assumption 2 is true for the numerical solution at time  $t_{n+1}$ .

**Remark 9.** By Lemma 2, we only need to check condition (92). In fact, by equation (91), if

$$D(\rho)(t) = \det \left( \int_{\Omega_x} \nabla \rho(x, t) (\nabla \rho(x, t))^T dx \right) > 0, \quad \forall 0 \leq t \leq T \quad (93)$$

where  $\rho$  is the diffusion limit, then for  $t_n$ , if  $\Delta x$  is small enough,  $\mathcal{H}(k^n)$  is very close to  $D(\rho)(t_n)$ . Therefore, (93) implies

$$\det(\mathcal{H}(k^n)) > 0. \quad (94)$$

In fact, to satisfy (93), it is sufficient to have

$$\int_{\Omega_x} |\nabla_r \rho(x, t)|^2 dx > 0, \quad \forall r \in \mathcal{S}^d, \quad 0 < t < T \quad (95)$$

where  $\nabla_r$  is directional derivative.

*Proof.* We have

$$K^n = k^n (\alpha^n)^T - \epsilon \sum_{k=1}^d D_k k^n (\alpha^n)^T \Xi_{v_k}^n + O(\epsilon^2). \quad (96)$$

If Assumption 2 is true at time  $t_{n-1}$ , then, by using equations (66),(67), we can show that there exists an orthogonal matrix  $Q$  such that

$$K^n Q = k^n (\alpha^{n,*})^T - \epsilon \sum_{k=1}^d D_k k^n (\alpha^{n,*})^T \Xi_{v_k}^{n,*} + O(\epsilon^2). \quad (97)$$

By using equations (63) and (67), we can rewrite (97) as

$$K^n Q = \left( \sqrt{N_v} k^n, -\epsilon \frac{\sqrt{N_v}}{\sqrt{d}} D_1 k^n, \dots, -\epsilon \frac{\sqrt{N_v}}{\sqrt{d}} D_d k^n, \dots \right) + O(\epsilon^2). \quad (98)$$

We notice that  $X^n$  comes from QR decomposition of  $K^{n-1}$ . This implies that there exists an invertible matrix  $P \in \mathbb{R}^{r \times r}$  such that

$$X^n P^{-1} = (k^n, -D_1 k^{n-1}, \dots, -D_d k^{n-1}, \dots). \quad (99)$$

We define  $X^* = X^n P^{-1}$  and for any  $1 \leq k \leq d$ , we further define

$$A_{\partial_k}^* = (X^*)^T D_K X^*, \text{ then } A_{\partial_k}^n = P^T A_{\partial_k}^* P \quad (100)$$

and

$$A_\sigma^* = (X^*)^T \text{diag}(\sigma(\mathcal{X})) X^*, \text{ then } A_\sigma^n = P^T A_\sigma^* P. \quad (101)$$

Plugging equations (100),(101) into (89) and letting  $l^* = P \hat{l}^{n+1/3}$ , it suffices to show that

$$\mathcal{R}^* = (A_\sigma^* l^*, A_{\partial_1}^* l^*, \dots, A_{\partial_d}^* l^*) \quad (102)$$

has rank  $d+1$ . Now we divide the following proof into two steps:

**First step:**  $(l^*)_1 \gg 0$  If  $\Delta t$ ,  $\epsilon$  is small enough. Similar to equation (77), we have

$$S^n (V^n)^T = L^n = l_0^n e^T + O(\epsilon). \quad (103)$$

Combining equation (103) with (99), we get

$$\mathbf{X}^* P \mathbf{S}^n (\mathbf{V}^n)^T = \mathbf{K}^n (\mathbf{V}^n)^T = k^n (\alpha^n)^T (\mathbf{V}^n)^T, \quad (104)$$

where the second equality comes from equation (50). Then by using equation (63) and (66), we can replace  $\alpha^n, \mathbf{V}^n$  with  $\alpha^{n,*}, \mathbf{V}^{n,*}$ , which gives use

$$\mathbf{X}^* P \mathbf{S}^n (\mathbf{V}^n)^T = k^n (\alpha^{n,*})^T (\mathbf{V}^{n,*})^T = k^n e^T + O(\epsilon^2). \quad (105)$$

Plugging equation (103) into (105), we get

$$\mathbf{X}^* P l_0^n e^T = k^n e^T. \quad (106)$$

Because  $\mathbf{X}^*$  is also an invertible matrix and the first column of  $\mathbf{X}^*$  is  $k^n$ , we must have

$$(P l_0^n)_1 = 1 + O(\epsilon). \quad (107)$$

Recall that

$$(l^*)_1 = (P \hat{l}^{n+1/3})_1 = (P l_0^{n+1/3})_1 + O(\epsilon). \quad (108)$$

Similar to asymptotic analysis performed to obtain (39), we get

$$\begin{aligned} & \frac{\mathbf{L}_0^{n+1/3} e - \mathbf{L}_0^n e}{\Delta t} - \sum_{k=1}^d \mathbf{A}_{\partial_k}^n (\mathbf{A}_\sigma^n)^{-1} \mathbf{A}_{\partial_k}^n \frac{l_0^{n+1/3} + l_0^n}{2} e^T \Pi_{v_k}^2 e = 0 \\ \Rightarrow & \frac{l_0^{n+1/3} - l_0^n}{\Delta t} - \frac{1}{d} \sum_{k=1}^d \mathbf{A}_{\partial_k}^n (\mathbf{A}_\sigma^n)^{-1} \mathbf{A}_{\partial_k}^n \frac{l_0^{n+1/3} + l_0^n}{2} = 0, \end{aligned} \quad (109)$$

From (23) we further get

$$\|l_0^{n+1/3} - l_0^n\|_2 = O\left(\frac{\Delta t}{(\Delta x)^2}\right). \quad (110)$$

Combining (107), (108) with (110), we finally obtain

$$\left| \left( P \left( \hat{l}^{n+1/3} - l_0^n \right) \right)_1 \right| = O\left(\frac{\Delta t}{(\Delta x)^2}\right) + O(\epsilon) \Rightarrow (l^*)_1 > 1 - \left[ O\left(\frac{\Delta t}{(\Delta x)^2}\right) + O(\epsilon) \right] \gg 0, \quad (111)$$

where  $\frac{\Delta t}{(\Delta x)^2}, \epsilon$  have to be very small.

**Second step:  $\Gamma^*$  is invertible.** Now we can prove (92) by contradiction. If we assume there exists  $\gamma \in \mathbb{R}^{(d+1) \times 1}$  with  $\|\gamma\|_2 = 1$  such that

$$\mathcal{R}^* \gamma = 0 \Rightarrow \left( \mathbf{A}_\sigma^* \gamma_1 + \sum_{i=1}^d \mathbf{A}_{\partial_i}^* \gamma_{i+1} \right) l^* = 0. \quad (112)$$

Because  $D_k$  is discretized using centered differences,  $\mathbf{A}_{\partial_i}^*$  is skew-symmetric for each  $i$ . Therefore, from equation (112) we deduce

$$(l^*)^T \left( \mathbf{A}_\sigma^* \gamma_1 + \sum_{i=1}^d \mathbf{A}_{\partial_i}^* \gamma_{i+1} \right) l^* = 0 \Rightarrow \gamma_1 (l^*)^T \mathbf{A}_\sigma^* l^* = 0 \Rightarrow \gamma_1 = 0 \Rightarrow \sum_{i=1}^d \mathbf{A}_{\partial_i}^* l^* \gamma_{i+1} = 0, \quad (113)$$

since  $A_\sigma^*$  is discretized using centered differences. Besides, if  $D_k$  is discretized using centered difference, we have

$$F^T D_k G = -G^T D_k F \quad (114)$$

for any  $F, G \in \mathbb{R}^{N_x \times 1}$ . Plugging equation (114) into (101), we obtain

$$(A_{\partial_k}^*)_{i,j} = \begin{cases} 0, & 2 \leq i, j \leq d+1 \\ 0, & i = j \\ - (D_{i-1} k^{n-1})^T (D_k k^{n-1}), & j = 1, 2 \leq i \leq d+1 \end{cases} \quad (115)$$

for any  $1 \leq k \leq d$ . Consider the first column of  $A_{\partial_k}^*$  from equation (115). Since  $(l^*)_1 \gg 0$ , equation (112) implies

$$\mathcal{H}(k^{n-1}) \gamma_{(2:d+1)} = 0, \quad (116)$$

where  $\mathcal{H}$  defined in equation (90) and  $\gamma_{(2:d+1)} \in \mathbb{R}^{d \times 1}$  is the cutoff vector to  $\gamma$  defined as

$$(\gamma_{(2:d+1)})_i = \gamma_{i+1}, \quad 1 \leq i \leq d \quad (117)$$

Because equation (92) implies  $\mathcal{H}(k^{n-1})$  is an invertible matrix, this finally shows that  $\gamma_{(2:d+1)}$  has to be zero, which contradicts  $\|\gamma\|_2 = 1$ .  $\square$

DEPARTMENT OF MATHEMATICS, UNIVERSITY OF WISCONSIN-MADISON, MADISON, WI 53705, USA  
E-mail address: `zding49@math.wisc.edu`

DEPARTMENT OF MATHEMATICS, UNIVERSITY OF INNSBRUCK, INNSBRUCK, AUSTRIA.  
E-mail address: `lukas.einkemmer@uibk.ac.at`

DEPARTMENT OF MATHEMATICS, UNIVERSITY OF WISCONSIN-MADISON, MADISON, WI 53705, USA  
E-mail address: `qinli@math.wisc.edu`